City Research Online

City, University of London Institutional Repository

This is the draft version of the paper.

This version of the publication may differ from the final published version.

Why do financial markets asymmetrically smile? A simple formula in the multi-factor Heston model

Maria Cristina Recchioni

Department of Economics and Social Sciences

Università Politecnica delle Marche, Ancona, Italy

E-mail: m.c.recchioni@univpm.it

Gabriele Tedeschi

Department of Economics

Universitat Jaume I, Castellon, Spain

E-mail: gabriele.tedeschi@gmail.com

Michelle S. Ouellette

Self-employed

Cabrera Pinto 10, 38700 Santa Cruz de La Palma, Spain E-mail: msocommunications@gmail.com

Giulia Iori

City, University of London, Department of Economics

Northampton Square, London EC1V 0HB

E-mail:g.iori@city.ac.uk

Abstract

A simple approach to determining the Gaussian kernel that constitutes the backbone of the multi-factor Heston model is proposed based on a suitable expansion in powers of volatilities of volatilities. This analysis provides Black-Scholes-like formulas for pricing European vanilla options, allowing for accurate approximations of the option prices under the multi-factor Heston model up to volatilities of volatilities on the order of 50%. The analysis also leads to a simple formula for the implied volatility showing that changes in the convexity of the volatility smile are due only to price skewness, and an easy formula to reproduce volatility indices via the realized volatility. Interestingly, the variance of the Gaussian kernel is equal to the variance of the continuously compounded return in the case of the Heston model. The empirical analyses presented assess the potential of our approach to capture market distortions while adequately forecasting the dynamics of the VIX index.

1 Introduction

The well known Heston model (1993) provides a natural generalization to the Black and Scholes (1973) approach to option pricing by introducing a stochastic dynamics for the volatility of returns. While closed form analytical solutions for the price of European options under this model are available, they are given

in terms of integrals in the complex plane that need to be solved computationally. Analytical solutions have also been derived for various generalization of the original Heston model, such as affine one-factor and multi-factor stochastic volatility models with and without jumps. Far from being exhaustive, here we mention Heston-like models such as Duffie et al. (2000), Hagan et al. (2002), Christoffersen et al. (2009), Fatone et al. (2009, 2013), Fritz et al. (2011), Recchioni and Sun (2016), Cui et al. (2017) and Recchioni and Tedeschi (2017). Although numerical approximation for solving closed form solutions can be extremely powerful in terms of accuracy, in the context of Heston like models the integrals are often unstable and can be very time consuming to compute. Easy-to-implement analytical approximations have been recognized as valuable alternatives to numerical solutions as they can aid in understanding the analytical features of option pricing models while speeding up calibration with market-observed quantities. Specifically, analytical approximation can provide a clear link between the features of the model and the observed characteristics of the implied volatility surface which is of particular interest for practitioners. Analytical approximations have thus be developed and continue to be proposed. Lewis (2000) derived an asymptotic expansion of implied volatility for small values of the volatility of volatility (vol of vol). This was followed by Lee (2001), who obtained similar results assuming a slow mean reversion of volatility, while Fouque et al. (2000) assumed fast mean-reverting volatility. Hagan et al. (2002) developed the SABR model using singular perturbations. Many authors have derived an asymptotic expansion in a jump-diffusion stochastic volatility model (see Medvedev and Scaillet (2007), Berestycki et al. (2004)) and in multifactor local-stochastic volatility (see Lorig et al. (2017)), whereas others have suggested perturbation expansions using Malliavin calculus (see Benhamou et al. (2009) and Larsson (2012)). Kristensen and Mele (2011) and Drimus (2011) also derived analytical approximations of option prices based on diffusions. Nicolato and Sloth (2012) took a more general approach, studying similar expansions that allow for jumps and stochastic volatility. Much attention has also been devoted to approximating the risk-neutral density as proposed by Abadir and Rockinger (2003), Aït-Sahalia (2002), Egorov et al. (2003), and Yu (2007) and to analyzing the market price of volatility and volatility-of-volatility risks.

This paper contributes to this strand of the literature, proposing an analytical approximations based on the extraction of the Gaussian kernel involved in the multi-factor Heston model, via a "suitable" expansion in powers of vols of vols of the characteristic function. Our method provides an explicit generalization of the Black and Scholes formula for option prices and an intuitive explanations of the smile asymmetry. While it is common to justify the smile based on asymmetric and non-lognormal implied volatility distributions our paper provides an explicit formula linking the curvature of the smile to the skewness of the underline asset returns distribution. The main results of the paper are: (i) A representation formula for the conditional marginal density of the multi-factor Heston model that allows us to capture the Gaussian kernel underlying the multi-factor Heston model (Proposition 2.1). (ii) Explicit formulas to approximate the conditional marginal density of the multi-factor Heston model in term of a Gaussian kernel plus a suitable correction. (iii) Explicit formulas in a Black-Scholes style for European vanilla call and put options. These formulas satisfy the put-call parity equation and show the effect of vols of vols in pricing options (see Propositions 3.1 and 3.2). (iv) An explicit formula for the implied volatility that, in the case of the Heston model, allows us to clearly identify the effect of price skewness on the asymmetry of the volatility smile. The formula is consistent with the smile shapes observed in the literature, and can generate a concave smile for sufficiently large price skewness. (v) An easy to compute formula for the variance of the continuously compounded return in the case of the Heston model.

We test, in Section 4, the accuracy of our analytical approximation, via simulations, by comparing our approximated second order Black and Scholes like approximations to the exact option values derived via numerical integration of the Recchioni and Sun (2016) formula, using two sets of parameters: First, we select several thousand values of the model parameters, moneyness, and time to maturity on a "reasonable" grid. The results (Subsection 4.1), for the case of the Heston model, show that at worst, four correct significant digits are always guaranteed by our approximation, for values of the vol of vol up to fifty per cent with maturity up to two years, while moneyness, E/S_0, lies in the range [0.8, 1.2] (see, Table 1). Second, we use the annual estimates of Heston and double Heston model parameters provided by Christoffersen et al. (2009). We show (Subsection 4.2) that, on average, the relative errors of the analytical approximation are few percents in the case of the Heston model and about 10% in the case of the double Heston model.

We test, in Section 5, the performance of our analytical approximation by running two empirical exercises: first, we compare the analytical approximation of the variance of the Gaussian Kernel, that in the Heston model coincides with the variance of compounded returns, calibrated to the U.S. S&P 500 index, and using the model parameters provided by Christoffersen et al. (2009), to the dynamics of the VIX index. We show in Subsection 5.1 that the Kernel variance is able to closely mimic the VIX behavior, and the fit compares favourably with the model of Corsi et al. (2013).
Second, we calibrate the Heston model parameters using the implied volatility formula derived via our analytical approximation and compare the second-order approximations for the Put and Call option prices to the respective option market prices on the same day and a day ahead. We show in Subsection 5.2 that the relative errors for the call options compares favourably with the literature (see, for example, Pacati et al. 2018).

The rest of this paper is organized as follows. In Section 2 we present the multi-factor Heston model and the main results. In Section 3 we show two applications of the results of Section 2 in computing option prices, implied volatility and interpreting the asymmetry of the implied volatility. In Section 4 we present a simulation study and in Section 5 empirical analyses to assess the performance of the approximations of the option prices. Section 6 concludes. The proofs of the main results are given in the Appendix A while in Appendix B we report some formulas for option pricing and tables.

2 Multi-factor Heston model treatment

We consider the following stochastic volatility model:

$$dx_t = \left(r(t) - \frac{1}{2} \sum_{j=1}^{n} v_{j,t} \right) dt + \sum_{j=1}^{n} \sqrt{v_{j,t}} dZ_{j,t}, \ \ t > 0, \tag{1}$$

$$dv_{j,t} = \chi_j(v_j^* - v_{j,t})dt + \gamma_j \sqrt{v_{j,t}} dW_{j,t}, \ \ t > 0, \tag{2}$$

where x_t denotes the log-price variable and $v_{1,t}, \ldots, v_{n,t}$ the corresponding variances, while $r(t)$ is the instantaneous risk free rate (assumed known in advance) and χ_j, v_j^*, γ_j are positive constants, and $Z_{j,t}$, $W_{j,t}$, $j = 1, 2, \ldots, n$, are standard Wiener processes such that all correlations among the Wiener processes are zero except for $E(dZ_{j,t}, dW_{j,t}) = \rho_j dt$, with constant correlation coefficients $\rho_j \in (-1, 1)$, $j = 1, 2, \ldots, n$.

Dividends are not included. The system of equations (1)-(2) is equipped with the following initial conditions:

$$x_0 = \log S_0^*, \tag{3}$$

$$v_{j,0} = v_{j,0}^*, \tag{4}$$

where S_0^* and $v_{j,0}^*$, $j = 1, 2, \ldots, n$ are the initial spot price and volatilities respectively, which are assumed to be random variables concentrated at a point with probability one.

As specified in Heston (1993), the quantity χ_j is the speed of mean reversion, v_j^* is the long-term mean, and γ_j is the local variance (volatility of volatility). These parameters are assumed to be positive so the process will be well defined.

It is worth noting that if the Feller condition is being enforce, i.e. $2\chi_j v_j^* / \gamma_j^2 > 1$, the variance $v_{j,t}$ is positive for any $t > 0$ with probability one (stationary volatility) and $v_{j,0} = v_{j,0}^* > 0$, $j = 1, 2, \ldots, n$ (see Revuz and Yor [25, Chapter XI] for the Bessel process).

Furthermore, we use $\underline{\gamma}$, $\underline{v}$ to denote the vectors containing the vols of vols, $\underline{\gamma} = (\gamma_1, \gamma_2, \ldots, \gamma_n)$, and the variances, $\underline{v} = (v_1, v_2, \ldots, v_n)$, respectively. The transition probability density function (pdf for short) associated with the stochastic differential system (1), (2) is denoted by $p_f(x, \underline{v}, t, x', \underline{v}', t')$, $(x, \underline{v})$, $(x', \underline{v}') \in \mathbb{R} \times \mathbb{R}^{n^+}$, t, $t' \geq 0$, $t' - t > 0$, where $\mathbb{R}$ denotes the set of real numbers, $\mathbb{R}^n$ the n-dimensional Euclidean vector space, and $\mathbb{R}^{n^+}$ the positive orthant.

The multi-factor Heston model is due to Christoffersen et al. (2009) and the analytical treatment under the assumptions $E(dW_{i,t}, dW_{j,t}) = 0$ and $E(dZ_{i,t}, dW_{j,t}) = 0$, $i \neq j$ is due to Fatone et al. (2009, 2013). The most commonly used model is the double Heston model (i.e., $n = 2$) in that it has proven to be very efficient in computing option prices and capturing volatility dynamics (see, for example, Christoffersen et al. 2009; Fatone et al. 2009, 2013; Recchioni and Sun 2016; Pacati et al. 2018).

In the following we illustrate the main contribution of the paper, which is to provide a representation formula for the conditional marginal density of the multi-factor Heston model, a key ingredient in the computation of the value of European call and put options. The representation allows us to extract the Gaussian kernel underlying the multi-factor Heston model (Proposition 2.1). Specifically, by denoting with $\mathcal{G}_\Gamma$ the Gaussian kernel with variance Γ, that is:

$$\mathcal{G}_\Gamma(y, t, t') = \frac{1}{\sqrt{2\pi\Gamma(t,t')}} e^{-\frac{1}{2\Gamma(t,t')} \left(y - \int_t^{t'} r(s)ds + \frac{1}{2}\Gamma(t,t') \right)^2}, \tag{5}$$

Propositions 2.2, 2.3 and 2.4 that follow show three Gaussian kernels associated with the multi-Heston volatility model: the zero-order kernel $\mathcal{G}_{\Gamma_0}$, the first-order kernel $\mathcal{G}_{\Gamma_1}$, and the second-order kernel $\mathcal{G}_{\Gamma_2}$. The terms "zero", "first", and "second order" refer to the fact that we use the first three terms of a suitable expansion in powers of vols of vols as they approach zero to determine these kernels. Specifically, Propositions 2.1 and 2.2 provide representation formulas for the marginal probability density of the log-price variable x_t conditioned to $\underline{v}_t = \underline{v}$. This representation allows us to provide explicit formulas to approximate the conditional marginal density of the multi-factor Heston model in term of the Gaussian kernel plus a suitable correction as proposed in Propositions 2.3 and 3.1. The main advantage of this analysis is that it enables the derivation of Black-Scholes-like formulas to price European vanilla options under the multi-Heston model, as shown in the next session.

We start with Proposition 2.1, which provides two representation formulas for the above-mentioned marginal density. These two formulas highlight the effect of the vols of vols γ_j, $j = 1, 2, \ldots, n$.

Proposition 2.1 *The marginal probability density of the log-price variable conditioned to* $\underline{v}_t = \underline{v}$ *is given by*

$$M(x,\underline{v},t,x',t') = \int_{\mathbb{R}^{n^+}} p_f(x,\underline{v},t,x',\underline{v}',t')d\underline{v}' = \frac{1}{2\pi}\int_{-\infty}^{+\infty} e^{\imath k(x'-x)-\imath k \int_t^{t'} r(s)ds+Q(t',t,\underline{v},k;\underline{\Theta}_v)}dk,$$

$$x,\, x' \in \mathbb{R},\; \underline{v} \in \mathbb{R}^{n^+},\, t, t' \geq 0, t'-t > 0, \tag{6}$$

where $\imath$ is the imaginary unit, $\underline{\Theta}_v$ is a vector containing the model parameters, and Q is the elementary function given by

$$Q(t',t,\underline{v},k;\underline{\Theta}_v) = \sum_{j=1}^n \int_t^{t'} E(v_{j,s}\,|\,\mathcal{F}_t)\left[\frac{1}{4}\gamma_j^2 B_j^2(k,s,t') + \imath k\,\rho_j\gamma_j B_j(k,s,t') - \frac{1}{2}(k^2 - \imath k)\right]ds. \tag{7}$$

where the conditional mean of the point-in-time volatility is given by

$$E(v_{j,t'}|\mathcal{F}_t) = v_{j,t}e^{-\chi_j(t'-t)} + v_j^*(1-e^{-\chi_j(t'-t)}), \quad t < t',$$

and $\mathcal{F}_t$ is the information set, i.e., the continuous σ-algebra generated by the point-in-time volatility processes.

Here, B_j *is given by*

$$B_j(k,t,t') = \frac{1}{2}(k^2 - \imath k)\frac{1-e^{-2\zeta_j(t'-t)}}{(\zeta_j+\nu_j)+(\zeta_j-\nu_j)e^{-2\zeta_j(t'-t)}}, \tag{8}$$

where ζ_j and ν_j are the following quantities:

$$\zeta_j(k) = \frac{1}{2}\left(4\nu_j^2 + \gamma_j^2(k^2 - \imath k)\right)^{1/2}, \tag{9}$$

$$\nu_j(k) = \frac{1}{2}(\imath k\rho_j\gamma_j + \chi_j). \tag{10}$$

Furthermore, the function M can be expressed as

$$M(x,\underline{v},t,x',t') =$$

$$\frac{1}{2\pi}\int_{-\infty}^{+\infty} \underbrace{e^{\imath k\left[(x'-x)-\int_t^{t'} r(s)ds+\frac{1}{2}\Gamma_0(t,t')\right]-\frac{1}{2}\Gamma_0(t,t')k^2}}_{Gaussian\,kernel}\underbrace{e^{\sum_{j=1}^n \int_t^{t'} E(v_{j,s}\,|\,\mathcal{F}_t)\left[\frac{\gamma_j^2}{2}B_j^2(k,s,t')+\imath k\rho_j\gamma_j B_j(k,s,t')\right]ds}}_{contribution\,from\,vols\,of\,vols}dk,$$

$$x,\, x' \in \mathbb{R},\; \underline{v} \in \mathbb{R}^{n^+},\, t,t' \geq 0, t'-t > 0, \tag{11}$$

that is,

$$M(x,\underline{v},t,x',t') = \int_{-\infty}^{+\infty} \mathcal{G}_{\Gamma_0}(x'-x-y,t,t')\mathcal{L}_{\underline{\gamma}}(y,t,t')dy, \tag{12}$$

where $\Gamma_0(t,t')$ is the integrated conditional variance:

$$\Gamma_0(t,t') = \sum_{j=1}^n \int_t^{t'} E(v_{j,s}\,|\,\mathcal{F}_t)ds, \tag{13}$$

while $\mathcal{G}_{\Gamma_0}$ is the Gaussian kernel in (5), and $\mathcal{L}_{\underline{\gamma}}$ is the function that accounts for the effects of the vols of vols:

$$\mathcal{L}_{\underline{\gamma}}(y,t,t') = \frac{1}{2\pi}\int_{-\infty}^{\infty} e^{\imath k y}e^{\sum_{j=1}^n \int_t^{t'} E(v_{j,s}\,|\,\mathcal{F}_t)\left[\frac{\gamma_j^2}{2}B_j^2(k,s,t')+\imath k\rho_j\gamma_j B_j(k,s,t')\right]ds}dk. \tag{14}$$

5

Proof of Proposition 2.1 *See Appendix A.*

Proposition 2.1 derives a formula (see Eq. (11)) in which the conditional marginal probability density of the log-price variable under the multi-factor Heston model is written in terms of the Gaussian kernel $\mathcal{G}_-$, and the effect of the vols of vols is highlighted with the function $\mathcal{L}_{\underline{\gamma}}$. It is worth noting that $\mathcal{L}_{\underline{\gamma}}$ satisfies the following equations:

$$\int_{-\infty}^{+\infty} dy \mathcal{L}_{\underline{\gamma}}(y,t,t') = 1 \quad t, t' > 0, \ t < t', \tag{15}$$

$$\int_{-\infty}^{+\infty} dy \, e^y \, \mathcal{L}_{\underline{\gamma}}(y,t,t') = 1 \quad t, t' > 0, \ t < t. \tag{16}$$

Eq. (15) guarantees that the conditional marginal density sums to one, while Eq. (16) guarantees that the multi-factor Heston process is a martingale. Eq. (16) holds since $B_j(k,t,t') = 0$ when $k = \imath, \ j = 1,2,\ldots,n$, as already stressed by Lewis (2000) Chp. 2, where conditions to avoid norm-defecting and martingale-defecting pdfs are discussed. Thus, any approximation of $\mathcal{L}_{\underline{\gamma}}$ must guarantee the above-mentioned conditions. We also check for the following condition satisfied by M:

$$\int_{-\infty}^{+\infty} \left(x' - x - \int_t^{t'} r(s)ds + \frac{1}{2}\Gamma_0(t,t') \right) M(x,\underline{v},t,x',t')dx' = 0. \tag{17}$$

We refer to Eq. (17) as the "symmetry condition". Proposition 2.2 investigates the effect of the vols of vols by looking at $\mathcal{L}_{\underline{\gamma}}$ in (14) and B_j in (8) in order to rewrite the marginal density in terms of a Gaussian kernel involving a first-order contribution in powers of the vols of vols.

Proposition 2.2 *The following expansion of the conditional marginal M in (6) in powers of $\underline{\gamma}$ as $\|\underline{\gamma}\| \to 0$ holds:*

$$M(x,\underline{v},t,x',t') \frac{1}{2\pi} \int_{-\infty}^{+\infty} \underbrace{e^{\imath k \left[(x'-x) - \int_t^{t'} r(s)ds + \frac{1}{2}\Gamma_1(t,t') \right] - \frac{1}{2}\Gamma_1(t,t')k^2}}_{Gaussian\ kernel} \underbrace{e^{S_1(t,t')(\imath k^3 + \imath k)}}_{Airy\ contribution} dk + o\left(\|\underline{\gamma}\|\right)$$

$$= \int_{-\infty}^{+\infty} \mathcal{G}_{\Gamma_1}(x' + S_1(t,t') - x - y,t,t')\mathcal{A}_{S_1}(y,t,t')dy + o\left(\|\underline{\gamma}\|\right)$$

$$= \int_{-\infty}^{+\infty} \mathcal{G}_{\Gamma_1}(x' - x - y,t,t')\mathcal{A}_{S_1}(y + S_1(t,t'),t,t')dy + o\left(\|\underline{\gamma}\|\right), \ \|\underline{\gamma}\| \to 0, \tag{18}$$

where S_1 and Γ_1 are defined as

$$S_1(t,t') = \frac{1}{2}\sum_{j=1}^{n} \frac{\rho_j \gamma_j}{\chi_j} \int_t^{t'} E(v_{j,s} \,|\, \mathcal{F}_t)\left(1 - e^{-\chi_j(t'-s)}\right) ds, \tag{19}$$

and

$$\Gamma_1(t,t') = \Gamma_0(t,t') - 2S_1(t,t'), \tag{20}$$

while $\mathcal{G}_{\Gamma_1}$ is the Gaussian kernel in (5) and $\mathcal{A}_{S_1}$ is the Airy function (see, Craig and Goodman (1990) and Vallée and Soares, 2004) with parameter S_1 defined as

$$\mathcal{A}_{S_1}(y) = \frac{1}{2\pi}\int_{-\infty}^{+\infty} e^{\imath k y} e^{S_1(t,t')\imath k^3} dk. \tag{21}$$

Proof of Proposition 2.2 *See Appendix A.*

6

Proposition 2.2 proves that the first-order expansion of the conditional marginal density M of the multi-factor Heston model is given by the convolution of a Gaussian kernel with a translated Airy function that converges to the Dirac delta function as $S_1(t, t')$ approaches zero. So, roughly speaking, the support of the Airy function $\mathcal{A}_{S_1}$ measures the deviation of the marginal density M from the Gaussian kernel G_{Γ_1} for small vols of vols. By approximating the Airy contribution in Eq. (21) for small values of $S_1(t, t')$ (that, as we will show in the next session, in the Heston model is related to the skew asymmetry), we therefore obtain one of the main formulas of this paper (i.e., Eq. (23)):

Proposition 2.3 *The following expansion of the conditional marginal M in (6) in powers of $\underline{\gamma}$ as $\|\underline{\gamma}\| \to 0$ holds:*

$$M(x, \underline{v}, t, x', t') = M_1(x, \underline{v}, t, x', t') + o\left(\|\underline{\gamma}\|\right), \quad \|\underline{\gamma}\| \to 0, \tag{22}$$

where M_1 is given by

$$M_1(x, \underline{v}, t, x', t') = \mathcal{G}_{\Gamma_1}(x' - x, t, t') + S_1(t, t') \left[-\frac{d^3 \mathcal{G}_{\Gamma_1}}{dx'^3}(x' - x, t, t') + \frac{d\mathcal{G}_{\Gamma_1}}{dx'}(x' - x, t, t') \right]. \tag{23}$$

Here, Γ_1 is defined in (20), $\mathcal{G}_{\Gamma_1}$ is the Gaussian kernel defined in (5), and S_1 is given in (19). We have

$$\int_{-\infty}^{+\infty} M_1(x, \underline{v}, t, x', t') dx' = 1, \tag{24}$$

$$\int_{-\infty}^{+\infty} e^{x'} M_1(x, \underline{v}, t, x', t') dx' = e^x, \tag{25}$$

and

$$\int_{-\infty}^{+\infty} \left(x' - x - \int_t^{t'} r(s) + \frac{1}{2}\Gamma_0(t, t') \right) M_1(x, \underline{v}, t, x', t') dx' = 0. \tag{26}$$

Proof of Proposition 2.3 *See Appendix A.*

We now complete the extraction by computing the second-order term of the expansion in powers of vols of vols of the exponent in formula (11).

Proposition 2.4 *The following expansion of the conditional marginal M in (6) in powers of $\underline{\gamma}$ as $\|\underline{\gamma}\| \to 0$ holds:*

$$M(x, \underline{v}, t, x', t') = M_2(x, \underline{v}, t, x', t') + o\left(\|\underline{\gamma}\|\right), \quad \|\underline{\gamma}\| \to 0, \tag{27}$$

M where M_2 is given by

$$M_2(x, \underline{v}, t, x', t') = \mathcal{G}_{\Gamma_2}(x' - x, t, t') + S_1(t, t') \left[-\frac{d^3 \mathcal{G}_{\Gamma_2}}{dx'^3}(x' - x, t, t') + \frac{d\mathcal{G}_{\Gamma_2}}{dx'}(x' - x, t, t') \right]$$

$$+ S_2(t, t') \left[\frac{d^4 \mathcal{G}_{\Gamma_2}}{dx'^4}(x' - x, t, t') + 2\frac{d^3 \mathcal{G}_{\Gamma_2}}{dx'^3}(x' - x, t, t') - \frac{d\mathcal{G}_{\Gamma_2}}{dx'}(x' - x, t, t') \right]$$

$$+ S_{2c}(t, t') \left[\frac{d^4 \mathcal{G}_{\Gamma_2}}{dx'^4}(x' - x, t, t') + \frac{d^3 \mathcal{G}_{\Gamma_2}}{dx'^3}(x' - x, t, t') \right]$$

$$+ \frac{1}{2} S_1^2(t, t') \left[\frac{d^6 \mathcal{G}_{\Gamma_2}}{dx'^6}(x' - x, t, t') - 2\frac{d^4 \mathcal{G}_{\Gamma_2}}{dx'^4}(x' - x, t, t') + \frac{d^2 \mathcal{G}_{\Gamma_2}}{dx'^2}(x' - x, t, t') \right]. \tag{28}$$

Here, S_1 is given by (19), $\mathcal{G}_{\Gamma_2}$ is the Gaussian kernel defined in (5), and S_2, S_{2c} and Γ_2 are defined as:

$$S_2(t,t') = \sum_{j=1}^{n} \frac{\gamma_j^2}{8\chi_j^2} \int_t^{t'} E(v_{j,s} \,|\, \mathcal{F}_t) \left(1 - e^{-\chi_j(t'-s)} \right)^2 ds, \tag{29}$$

$$S_{2c}(t,t') = \sum_{j=1}^{n} \frac{\gamma_j^2 \rho_j^2}{2\chi_j} \int_t^{t'} E(v_{j,s} \,|\, \mathcal{F}_t) e^{-\chi_j(t'-s)} \int_s^{t'} \left(e^{\chi_j(t'-\tau)} - 1 \right) d\tau \, ds, \tag{30}$$

and

$$\Gamma_2(t,t') = \Gamma_0(t,t') - 2S_1(t,t') + 2S_2(t,t') = \Gamma_1(t,t') + 2S_2(t,t'), \tag{31}$$

where Γ_1 is given in (20).

Furthermore, we have

$$\int_{-\infty}^{+\infty} M_2(x, \underline{v}, t, x', t') dx' = 1, \tag{32}$$

and

$$\int_{-\infty}^{+\infty} e^{x'} M_2(x, \underline{v}, t, x', t') dx' = e^x. \tag{33}$$

$$\int_{-\infty}^{+\infty} \left(x' - x - \int_t^{t'} r(s) ds + \frac{1}{2} \Gamma_0(t,t') \right) M_2(x, \underline{v}, t, x', t') dx' = 0. \tag{34}$$

Proof of Proposition 2.4 *See Appendix A.*

We note that the integrals appearing in Γ_1 and Γ_2 can be computed explicitely and are elementary functions of time.

Let us now comment on this result. First, it is worth noting that the Gaussian kernel $\mathcal{G}_{\Gamma_2}$ is the "backbone" of the multi-factor Heston model in that we cannot extract a Gaussian kernel different from $\mathcal{G}_{\Gamma_2}$ proceeding further in the expansion of the conditional marginal M in powers of vols of vols.

Second, in the Heston framework, the variance $\Gamma_2(t,T)$ is the variance of of the continuously compounded return R_t^T:

$$R_t^T = \log \left(\frac{S_T}{S_t} \right), \tag{35}$$

while the quantities S_1 and S_2 are related to the processes X_T and Y_T defined by

$$X_T = \int_t^T \sqrt{v_s} dZ_s \quad \text{and} \quad Y_T = \int_t^T [v_s - E_t(v_s)] ds. \tag{36}$$

Here, $E_t(\cdot) = E(\cdot \,|\, \mathcal{F})$ to keep the notation simple. This finding is based on the following result of Zhang et al. (2017):

$$E_t([R_t^T - E_t(R_t^T)]^2) = E_t(X_T^2) - E_t(X_T Y_T) + \frac{1}{4} E_t(Y_T^2), \tag{37}$$

where

$$E_t(X_T^2) = \int_t^T E_t(v_s) ds, \quad E_t(X_T^3) = 3 \frac{\rho\gamma}{\chi} \int_t^T E_t(v_s)(1 - e^{-\chi(T-s)}) ds, \tag{38}$$

$$E_t(X_T Y_T) = \frac{\rho\gamma}{\chi} \int_t^T E_t(v_s)(1 - e^{-\chi(T-s)}) ds \quad \text{and} \quad E_t(Y_T^2) = \frac{\gamma^2}{\chi^2} \int_t^T E_t(v_s)(1 - e^{-\chi(T-s)})^2 ds. \tag{39}$$

Bearing in mind that $E_t(v_s) = E(v_s \,|\, \mathcal{F}_t) = v^* + (v_t - v^*)e^{-\chi(s-t)}$ and given the expressions for Γ_0, S_1, S_2 in Eqs. (13), (19), and (29) we have:

$$E_t([R_t^T - E_t(R_t^T)]^2) = E_t(X_T^2) - E_t(X_T Y_T) + \frac{1}{4}E_t(Y_T^2) = \Gamma_0(0,T) - 2S_1(0,T) + 2S_2(0,T), \qquad (40)$$

and

$$E_t(X_T^2) = \Gamma_0(t,T), \quad E_t(X_T^3) = 6S_1(t,T), \quad E_t(X_T Y_T) = 2S_1(t,T), \quad E_t(Y_T^2) = 8S_2(t,T). \qquad (41)$$

Third, using the price skewness formula from Das and Sundaram (1999),

$$\text{Skewness}_{DS} = \frac{E_t(X_T^3)}{\left[X_T^2\right]^{3/2}} = 6\frac{S_1(t,T)}{\Gamma_0(t,T)^{3/2}}, \qquad (42)$$

we see that this quantity appears in the coefficient of the second-order term of the implied volatility in Eq. (70).

Propositions 2.3 and 2.4 are the main results of this paper since they may have several applications, including the calibration of the Heston model and multi-factor Heston model on asset pricing. In the following, we focus on two main applications. The first is the approximation of the European vanilla option prices under the multi-factor Heston model. The second is a second-order expansion of the implied volatility in powers of vols of vols.

3 Applications of the multi-factor Heston kernel approximations

3.1 Option pricing

In this section we derive explicit formulas for European vanilla call and put options by using the first-order, M_1, and second-order, M_2, approximations for the multi-factor Heston conditional marginal, M.

In the following, we use $C_{MH}(S_0, T, E)$ and $P_{MH}(S_0, T, E)$ to denote the price of European vanilla call and put options, respectively, in the multi-factor Heston model, with spot price S_0, maturity T, strike price E, and discount factor $B(T)$, which is given by

$$B(T) = e^{-\int_0^T r(s)ds}. \qquad (43)$$

Specifically, C_{MH} and P_{MH} read as:

$$C_{MH}(S_0, T, E) = B(T) \int_{\log E}^{+\infty} (e^{x'} - E)M(\log S_0, \underline{v}_0, 0, x', T)dx', \qquad (44)$$

and

$$P_{MH}(S_0, T, E) = B(T) \int_{-\infty}^{\log E} (E - e^{x'})M(\log S_0, \underline{v}_0, 0, x', T)dx', \qquad (45)$$

where $\underline{v}_0$ is the vector of the variances at time $t = 0$.

Furthermore, we use $C_{BS}\left(S_0, T, E, \sqrt{\frac{\Gamma}{T}}\right)$ and $P_{BS}\left(S_0, T, E, \sqrt{\frac{\Gamma}{T}}\right)$ to denote the classical Black-Scholes formulas for call and put vanilla options, where $\Gamma = \Gamma(0,T) > 0$ is the integrated variance over the time interval $[0, T]$, that is,

$$C_{BS}\left(S_0, T, E, \sqrt{\frac{\Gamma}{T}}\right) = S_0 N(d_1(\Gamma)) - Ee^{-\int_0^T r(s)ds}N(d_2(\Gamma)), \qquad (46)$$

9

and

$$P_{BS}\left(S_0, T, E, \sqrt{\frac{\Gamma}{T}}\right) = -S_0 N(-d_1(\Gamma)) + Ee^{-\int_0^T r(s)ds} N(-d_2(\Gamma)), \tag{47}$$

where $N(x)$ ia given by

$$N(x) = \frac{1}{\sqrt{2\pi}} \int_{-\infty}^x e^{-y^2/2} dy, \tag{48}$$

and $d_1(\Gamma)$ and $d_2(\Gamma)$ are given by

$$d_1(\Gamma) = \frac{\log\left(\frac{S_0}{E}\right) + \int_0^T r(s)ds + \frac{1}{2}\Gamma}{\sqrt{\Gamma}}, \tag{49}$$

$$d_2(\Gamma) = d_1(\Gamma) - \sqrt{\Gamma} = \frac{\log\left(\frac{S_0}{E}\right) + \int_0^T r(s)ds - \frac{1}{2}\Gamma}{\sqrt{\Gamma}}. \tag{50}$$

Proposition 3.1 *Let C_{MH}, P_{MH} be the prices of European call and put options with spot price S_0, maturity T, strike price E, and discount factor $B(T)$ as given in Eqs. (44)–(45). Assuming $\Gamma_1(0,T) > 0$ in Eq. (20), we have*

$$C_{MH}(S_0, T, E) = C_{BS}\left(S_0, T, E, \sqrt{\frac{\Gamma_1}{T}}\right) + \mathcal{R}_{1,MH}(S_0, T, E) + o\left(\|\underline{\gamma}\|\right), \ \|\underline{\gamma}\| \to 0,$$
$$S_0 > 0, \ T > 0, \ E > 0, \tag{51}$$

and

$$P_{MH}(S_0, T, E) = P_{BS}\left(S_0, T, E, \sqrt{\frac{\Gamma_1}{T}}\right) + \mathcal{R}_{1,MH}(S_0, T, E) + o\left(\|\underline{\gamma}\|\right), \ \|\underline{\gamma}\| \to 0,$$
$$S_0 > 0, \ T > 0, \ E > 0. \tag{52}$$

Here, C_{BS} and P_{BS} denote the classical Black-Scholes formulas given in (46) and (47). In turn, $\mathcal{R}_{1,MH}$ is the correction to the standard Black-Scholes formula due to the contribution of the zero and first-order terms of the kernel expansion in powers of vols of vols:

$$\mathcal{R}_{1,MH}(S_0, T, E) = B(T)E\frac{S_1(0,T)}{\Gamma_1(0,T)}\left(m_E + \frac{3}{2}\Gamma_1(0,T)\right)\mathcal{G}_{\Gamma_1}(\ln(E/S_0), 0, T), \tag{53}$$

where m_E is the log-moneyness associated with the forward price defined as

$$m_E = \log\left(\frac{E}{S_0 e^{\int_0^T r(s)ds}}\right). \tag{54}$$

Proof of Proposition 3.1 *See Appendix A.*

The correction term $\mathcal{R}_{1,MH}$ can be rewritten in a more standard form

$$\mathcal{R}_{1,MH}(S_0, T, E) = Ee^{-\int_0^T r(s)ds} N'(d_2(\Gamma_1))\frac{S_1(0,T)}{\Gamma_1(0,T)}\left(-d_2(\Gamma_1) + \sqrt{\Gamma_1(0,T)}\right), \tag{55}$$

10

where $N'(\cdot)$ represents the derivatives of $N(\cdot)$ defined in (48) and d_2 is given in (50). Bearing in mind that $S_0 N'(d_1(\Gamma)) = E e^{-\int_0^T r(s)ds} N'(d_2(\Gamma))$ for any positive Γ, and that the Black-Scholes Vega is $Vega = Vega(\Gamma) = \sqrt{T} S_0 N'(d_1(\Gamma))$, Eq. (55) can also be written as

$$
\begin{aligned}
\mathcal{R}_{1,MH}(S_0, T, E) &= S_0 N'(d_1(\Gamma_1)) \frac{S_1(0,T)}{\Gamma_1(0,T)} \left(-d_2(\Gamma_1) + \sqrt{\Gamma_1(0,T)} \right) \\
&= Vega(\Gamma_1) \frac{S_1(0,T)}{\sqrt{T}\Gamma_1(0,T)^{3/2}} \left(m_E + \frac{3}{2}\Gamma_1(0,T) \right).
\end{aligned}
\tag{56}
$$

We now show the approximation of the European call and put options when the kernel approximation M_2 of the conditional marginal M associated with the multi-factor Heston model is used.

Proposition 3.2 *Let C_{MH}, P_{MH} be the prices of European call and put options with spot price S_0, maturity T, strike price E and discount factor $B(T)$ as given in Eqs. (44)–(45). Assuming $\Gamma_2(0,T) > 0$ in Eq. (31), we have*

$$
C_{MH}(S_0, T, E) = C_{BS}\left(S_0, T, E, \frac{\sqrt{\Gamma_2}}{\sqrt{T}}\right) + \mathcal{R}_{2,MH}(S_0, T, E) + o\left(\|\underline{\gamma}\|\right), \quad \|\underline{\gamma}\| \to 0,
$$
$$
S_0 > 0, \, T > 0, \, E > 0
\tag{57}
$$

and

$$
P_{MH}(S_0, T, E) = P_{BS}\left(S_0, T, E, \frac{\sqrt{\Gamma_2}}{\sqrt{T}}\right) + \mathcal{R}_{2,MH}(S_0, T, E) + o\left(\|\underline{\gamma}\|\right), \quad \|\underline{\gamma}\| \to 0,
$$
$$
S_0 > 0, \, T > 0, \, E > 0.
\tag{58}
$$

Here, C_{BS} and P_{BS} denote the classical Black-Scholes formulas as in (46) and (47), while $\mathcal{R}_{2,MH}$ is the correction to the standard Black-Scholes formula due to the contribution of the zero, first- and second-order terms of the kernel expansion in powers of vols of vols:

$$
\mathcal{R}_{2,MH}(S_0, T, E) = B(T) E \frac{S_1(0,T)}{\Gamma_2(0,T)} \left(+\log\left(\frac{E}{S_0 e^{\int_0^T r(s)ds}}\right) + \frac{3}{2}\Gamma_2(0,T) \right) \mathcal{G}_{\Gamma_2}(\log(E/S_0), 0, T)
$$
$$
+ S_2(0,T) B(T) E \left[\frac{d^2 \mathcal{G}_{\Gamma_2}}{dx'^2} + \frac{d\mathcal{G}_{\Gamma_2}}{dx'} - \mathcal{G}_{\Gamma_2} \right] (\log(E/S_0), 0, T) + S_{2c}(0,T) B(T) E \frac{d^2 \mathcal{G}_{\Gamma_2}}{dx'^2}(\log(E/S_0), 0, T)
$$
$$
+ \frac{1}{2} S_1^2(0,T) B(T) E \left[\frac{d^4 \mathcal{G}_{\Gamma_2}}{dx'^4} - \frac{d^3 \mathcal{G}_{\Gamma_2}}{dx'^3} - \frac{d^2 \mathcal{G}_{\Gamma_2}}{dx'^2} + \frac{d\mathcal{G}_{\Gamma_2}}{dx'} \right] (\log(E/S_0), 0, T).
\tag{59}
$$

The notation $[\cdot](\cdot, \cdot, \cdot)$ in Eq. (59) means that the function in the square brackets is evaluated at the argument $(\cdot, \cdot, \cdot)$. Dropping the arguments of Γ_2, S_1, S_2 and S_{2c}, Eq. (59) also reads:

$$
\begin{aligned}
\mathcal{R}_{2,MH}(S_0, T, E) = &\frac{Vega(\Gamma_2)}{\sqrt{T}\Gamma_2^{3/2}} S_1 \left(m_E + \frac{3}{2}\Gamma_2 \right) + S_{2c} \frac{Vega(\Gamma_2)}{\sqrt{T}\,\Gamma_2^{3/2}} \left[\frac{(m_E + \frac{1}{2}\Gamma_2)^2}{\Gamma_2} - 1 \right] \\
&+ S_2 \frac{Vega(\Gamma_2)}{\sqrt{T}\,\Gamma_2^{3/2}} \left[\frac{(m_E + \frac{1}{2}\Gamma_2)^2}{\Gamma_2} - (m_E + \frac{1}{2}\Gamma_2) - 1 - \Gamma_2 \right] \\
&+ \frac{1}{2} S_1^2 \frac{Vega(\Gamma_2)}{\sqrt{T}\,\Gamma_2^{3/2}} \left[\frac{(m_E + \frac{1}{2}\Gamma_2)^4}{\Gamma_2^3} + \frac{(m_E + \frac{1}{2}\Gamma_2)^3}{\Gamma_2^2} - \frac{(m_E + \frac{1}{2}\Gamma_2)^2}{\Gamma_2}\left(1 + \frac{6}{\Gamma_2}\right) \right] \\
&+ \frac{1}{2} S_1^2 \frac{Vega(\Gamma_2)}{\sqrt{T}\,\Gamma_2^{3/2}} \left[-(m_E + \frac{1}{2}\Gamma_2)\left(1 + \frac{3}{\Gamma_2}\right) + \left(1 + \frac{3}{\Gamma_2}\right) \right],
\end{aligned}
\tag{60}
$$

where m_E is the log-moneyness associated with the forward price (see Eq. (54)).

Proof of Proposition 3.2 *See Appendix A.*

In the following, we approximate the European vanilla option prices using the first-order approximations:

$$C_{1,MH}(S_0, T, E) = C_{BS}\left(S_0, T, E, \frac{\sqrt{\Gamma_1}}{\sqrt{T}}\right) + \mathcal{R}_{1,MH}(S_0, T, E), \tag{61}$$

$$P_{1,MH}(S_0, T, E) = P_{BS}\left(S_0, T, E, \frac{\sqrt{\Gamma_1}}{\sqrt{T}}\right) + \mathcal{R}_{1,MH}(S_0, T, E), \tag{62}$$

and the second-order approximations:

$$C_{2,MH}(S_0, T, E) = C_{BS}\left(S_0, T, E, \frac{\sqrt{\Gamma_2}}{\sqrt{T}}\right) + \mathcal{R}_{2,MH}(S_0, T, E), \tag{63}$$

$$P_{2,MH}(S_0, T, E) = P_{BS}\left(S_0, T, E, \frac{\sqrt{\Gamma_2}}{\sqrt{T}}\right) + \mathcal{R}_{2,MH}(S_0, T, E). \tag{64}$$

In the following we refer to formulas $C_{1,MH}$ and $P_{1,MH}$ as the first-order Black-Scholes formulas for call and put options and $C_{2,MH}$ and $P_{2,MH}$ as the second-order Black-Scholes formulas. In the following we use the subscript "H" to denote the option prices and their approximation in the Heston framework and "DH" for the double Heston.

It is worth noting that:

(*i*) The Black-Scholes formulas for the European vanilla options overprice the at-the-money options. The first-order correction term $\mathcal{R}_{1,MH}$, which affects the call and put options in the same way, is able to correct for this overpricing. In fact, $\mathcal{R}_{1,MH}$ is negative when the options are at-the money (i.e., $E/(S_0 e^{\int_0^T r(s)ds}) \approx 1$) and the correlations are negative. This finding tells us that in the case of the Heston model where negative correlation values are usually observed, the prices of call and put options are smaller than those calculated using the standard Black-Scholes formulas for the at-the-money options, thereby reducing the overpricing of the Black-Scholes formulas.

(*ii*) The correction term, $\mathcal{R}_{1,MH}$, shows why S_1 may be considered to be responsible for smile asymmetry. In fact, when $\rho_j = 0$ to first order in γ_j, $j = 1, 2, \ldots, n$, we observe a volatility independent of moneyness defined with respect to the forward price (i.e., $E/(S_0 e^{\int_0^T r(s)ds})$), in contrast to the case $\rho_j \neq 0$, where we observe a dependence of the volatility on moneyness. Specifically, negative correlations imply negative corrections for moneyness larger than or equal to one, while the sign of the correction depends on the variance Γ_1 for moneyness smaller than one.

(*iii*) The correction terms $\mathcal{R}_{1,MH}$ and $\mathcal{R}_{2,MH}$ are the same for the call and put options. As a consequence, the pairs $C_{1,MH}$, $P_{1,MH}$ and $C_{2,MH}$, $P_{2,MH}$ satisfy the put-call parity. In fact $C_{j,MH} - P_{j,MH} = C_{BS}\left(S_0, T, E, \frac{\sqrt{\Gamma_j}}{\sqrt{T}}\right) - P_{BS}\left(S_0, T, E, \frac{\sqrt{\Gamma_j}}{\sqrt{T}}\right) = S_0 - E e^{\int_0^t r(s)ds}$, $j = 1, 2$.

(*iv*) The correction term $\mathcal{R}_{1,MH}$ is linear in the Vega of the Black-Scholes formulas (61) and (62) (see Eq. (56). Specifically, the ratio correction term for Vega depends linearly on S_1 and the log-moneyness, $\log\left(\frac{E}{S_0 e^{\int_0^T r(s)ds}}\right)$.

(v) The Gaussian kernel $\mathcal{G}_{\Gamma_2}$ is the backbone of the multi-factor Heston model in that we cannot extract a Gaussian kernel different from $\mathcal{G}_{\Gamma_2}$ proceeding further in the expansion of the conditional marginal M in powers of vols of vols. Thus, by continuing the expansion of M, we affect only the correction term of formulas $C_{2,a}$ and $P_{2,a}$.

3.2 Implied volatility

The implied volatility Σ in the multi-factor Heston model is defined as the quantity such that the following equality holds:

$$C_{BS}\left(S_0, T, E, \sqrt{\frac{\Sigma^2}{T}}\right) = C_{MH}(S_0, T, E), \tag{65}$$

where C_{BS} and C_{MH} are the prices at time $t = 0$ of a European call option with strike price $E > 0$, and maturity time $T > 0$ in the Black-Scholes and multi-factor Heston models, respectively.

We derive the first and second-order approximations of Σ as a function of the vols of vols (i.e., $\Sigma = \Sigma(\underline{\gamma})$) by using the expansion in powers of vols of vols as the vols of vols go to zero. Specifically, we look for the first-order approximation $\Sigma_{1,MH}$ by solving the equation

$$C_{BS}\left(S_0, T, E, \sqrt{\frac{\Sigma_{1,MH}^2(\underline{\gamma})}{T}}\right) = C_{BS}\left(S_0, T, E, \sqrt{\frac{\Gamma_1}{T}}\right) + \mathcal{R}_{1,MH}(S_0, T, E), \tag{66}$$

while we obtain the second-order approximation $\Sigma_{2,MH}$ by solving

$$C_{BS}\left(S_0, T, E, \sqrt{\frac{\Sigma_{2,MH}^2(\underline{\gamma})}{T}}\right) = C_{BS}\left(S_0, T, E, \sqrt{\frac{\Gamma_1}{T}}\right) + \mathcal{R}_{2,MH}(S_0, T, E). \tag{67}$$

It is easy to see that by solving Eq. (67) we also determine the first-order approximation $\Sigma_{1,MH}$.

Proposition 3.3 *The following expansion of implied volatility defined in Eq. (66) in powers of γ_j, $j = 1, 2, \ldots, n$, holds as $\gamma_j \to 0$ for the multi-factor Heston model:*

$$\Sigma(\underline{\gamma}) = \Sigma_{1,MH}(\underline{\gamma}) + o\left(\|\underline{\gamma}\|\right), \quad \|\underline{\gamma}\| \to 0, \tag{68}$$

where $\Sigma_{1,MH}$ is given by:

$$\Sigma_{1,MH}(\underline{\gamma}) = \sqrt{\Gamma_0} + \frac{S_1}{\Gamma_0\sqrt{\Gamma_0}}\left(m_E + \frac{1}{2}\Gamma_0\right) + o\left(\|\underline{\gamma}\|\right), \quad \|\underline{\gamma}\| \to 0, \tag{69}$$

where m_E is the log-moneyness associated with the forward price (see Eq. (54)). Here, we have dropped the arguments of the function Γ_0 and S_1 defined in (13) and (19).

The second-order approximation, $\Sigma_{2,MH}$, of Σ is given by

$$\Sigma_{2,MH}(\underline{\gamma}) = \sqrt{\Gamma_0} + \frac{1}{\Gamma_0\sqrt{\Gamma_0}}\left[a_2(T,\underline{\gamma})\left(m_E + \frac{1}{2}\Gamma_0\right)^2 + a_1(T,\underline{\gamma})\left(m_E + \frac{1}{2}\Gamma_0\right) + a_0(T,\underline{\gamma})\right], \tag{70}$$

where $a_0(T,\underline{\gamma})$, $a_1(T,\underline{\gamma})$ and $a_2(T,\underline{\gamma})$ are given by

$$a_0(T,\underline{\gamma}) = (1 + \frac{3}{2}\frac{1}{\Gamma_0})S_1^2 - S_2 - S_{2c}, \tag{71}$$

$$a_1(T, \underline{\gamma}) = S_1 - S_2 + \frac{3}{2} \frac{1}{\Gamma_0} S_1^2, \tag{72}$$

and

$$a_2(T, \underline{\gamma}) = \frac{1}{\Gamma_0} \left(S_2 + S_{2c} - \frac{3}{\Gamma_0} S_1^2 \right). \tag{73}$$

Here, we have dropped the arguments $(0, T)$ of the functions Γ_0, S_1, S_2 and S_{2c} given in (13), (19), (29), (30), respectively.

Proof of Proposition 3.3 *See Appendix A.*

It is worth noting that, while the correction $C_{2,MH}$ is a fourth-degree polynomial in moneyness, the implied volatility resulting from the second-order approximation to the option prices is a quadratic function of moneyness since suitable cancellations occur when computing the expansion of the implied volatility as the vols of vols go to zero. As a result, the coefficients $a_0(T, \underline{\gamma})$ and $a_2(T, \underline{\gamma})$ are second-degree homogeneous functions of $\underline{\gamma}$, while $a_1(T, \underline{\gamma})$ is a homogeneous function of degree one.

For null correlation coefficients, the second-order approximation, $\Sigma_{2,MH}$, of the volatility surface is a strictly convex function with vertex at $m_E = 0$ (i.e., when the option is at the money):

$$\Sigma_{2,MH}(\underline{\gamma}) = \sqrt{\Gamma_0} + \frac{S_2}{\Gamma_0 \sqrt{\Gamma_0}} \left[\frac{1}{\Gamma_0} \left(m_E + \frac{1}{2} \Gamma_0 \right)^2 - \left(m_E + \frac{1}{2} \Gamma_0 \right) - 1 \right]. \tag{74}$$

The expression of a_2 reveals that the convexity of the volatility smile depends on the function S_1^2. This finding confirms the fact that the quantity S_1 is responsible for asymmetry in the smile since it allows for concavity. Concave volatility smiles are allowed in mean-reverting underlying assets where the option tenor is comparable to the characteristic reversion time of the asset[*]. Furthermore, bearing in mind the price skewness by Das and Sundaram (1999) given in Eq. (42), the coefficient of the highest order term in Eq. (70) also reads:

$$\frac{1}{\Gamma_0^{3/2}} a_2(T, \underline{\gamma}) = \frac{1}{\Gamma_0^{1/2}} \left[\frac{1}{\Gamma_0^2} (S_2 + S_{2c}) - \frac{1}{12} \text{Skewness}_{DS}^2 \right]. \tag{75}$$

Eq. (75) clearly shows the effect of the price skewness on the volatility smile.

4   Accuracy of the Black-Scholes approximations: simulation study

In this section, we study the accuracy of the formulas derived in Sections 2 and 3 in reproducing the European option price and implied volatility in the Heston and multi-factor Heston models and their performance in terms of computational time. We compute the exact European option prices in the Heston/multi-Heston models by using the option price formulas proposed by Recchioni and Sun (2016) and reported in Appendix B. These formulas are integral representation formulas that differ only in the choice of a real parameter q, which should be larger than one to compute a call option and smaller than 0 to compute a put option. These formulas are in line with the Lewis regularization technique (i.e., Lewis 2000, Chap 2), whose integrand functions are smooth functions. In the following, we denote with $C_{MH}(S_0, T, E)$ and $P_{MH}(S_0, T, E)$ the prices of the European vanilla call and put options obtained by using formulas (147) and (148) in Appendix B.

---

[*]Some empirical evidence can be found at http://faculty.baruch.cuny.edu/jgatheral/Bachelier2008.pdf (see pages 53–56)

4.1 Simulation study 1: Heston on "reasonable" grid of parameters

This section is devoted to assessing the performance of the first- and second-order approximations $C_{1,MH}$, $P_{1,MH}$ (see Eqs. (61)–(62)) and $C_{2,MH}$, $P_{2,MH}$ (see Eqs. (63)–(64)) of the call and put option prices in the Heston framework (i.e., $n = 1$ in Eqs. (61)–(64)). This analysis is done to show that these first- and second-order Black-Scholes (BS for short in the following) approximations to option European vanilla option prices are of sufficient quality to be used for estimating the multi-factor Heston model parameters.

The Heston exact formula is obtained by imposing $n = 1$ in Eqs. (149) in Appendix B. As previously mentioned, Eqs. (147), (148) in Appendix B are equal except for the values of q, which are valid over different intervals. In the following, we choose $q = 3$ for a call option and $q = -2$ for a put option. Equations (147) and (148) are defined via convergent integrals that can be computed accurately using a simple composite rectangular rule with 2^{16} quadrature nodes. Obviously, depending on the choice of the model parameters and the time to maturity, the number of quadrature points could be reduced.

We evaluate the exact formulas C_H, P_H and the second-order Black-Scholes formulas $C_{j,H}$, $P_{j,H}$, for $j = 1, 2$ at the points in the following set:

$$
\begin{aligned}
\mathcal{M} = \{ \, (S_0, E, T, \gamma, v_0, \chi, v^*, \rho, r) \, | S_0 = 100, \, E = 80 + 10(j-1), \, T = 2\,j/5, \, j = 1, 2, \ldots, 5, \\
\gamma = 0.01, 0.05, 0.15, 0.25, 0.5, \, v_0 = 2 + j/5, j = 1, 2, \ldots, 5, \, \chi = 1.5 + 1.5(j-1), j = 1, 2, \ldots, 5, \\
v^* = j\,\gamma^2/(2\chi), \rho = -j/6, j = 1, 2, \ldots, 5, r = 0.01 \} \, .
\end{aligned}
\tag{76}
$$

These values of model parameters in the grid M include those estimated by Christoffersen et al. (2009) in Section 4.2 Table 3 (see Appendix B).

Figures 1 and 2 show the empirical distributions of the relative errors in call and put prices, $e_{C,j} = |C_H - C_{j,H}^j|/|C_H|$, $j = 1, 2$ (upper panels) and $e_{P,j} = |P_H - P_{j,H}|/|P_H|$, $j = 1, 2$ (lower panel), when $\gamma = 0.15$ (left panel), $\gamma = 0.25$ (middle panel), and $\gamma = 0.5$ (right panel) based on grid M. We observe that the second-order approximations $C_{2,H}$ and $P_{2,H}$ of the call and put option prices, respectively, strongly outperform the first-order approximations $C_{1,H}$ and $P_{1,H}$ in terms of accuracy for vols-of-vols larger than 10%.

To further investigate the quality of the option approximations shown in Table 1, the mean, median, and standard deviation of their relative errors for the same values of γ as mentioned above, as well as two additional values ($\gamma = 0.01$ and $\gamma = 0.05$) are shown in Table 1. From left to right, the Table shows the value of the vol of vol (γ), the mean (mean$_C$), median (median$_C$), and standard deviation (std$_C$) of the relative call option errors $e_{C,j}$ and the mean (mean$_P$), median (median$_P$), and standard deviation (std$_P$) of the relative put option errors $e_{P,j}$ associated with the first-order ($j = 1$, upper panel of Table 1) and second-order Black-Scholes formulas ($j = 2$, lower panel of Table 1). As well, some descriptive statistics for the call and put option prices are shown in Table 2. We conclude this section by showing the great savings in computing time resulting from the use of the second-order Black-Scholes formulas (63) and (64) with $n = 1$ derived here to approximate the option prices. To this end, the execution time (seconds) required to compute 40,000 European call and put options using Eqs. (147), (148) in the Heston model with the rectangular quadrature rule with N_p nodes, referred to as $Time_{true}$, is compared to the time $Time_{approx}$ required using Eqs.} (63) and (64) with $n = 1$. Table 3 also shows great savings in computer time when small N_p values are involved. That is, these second-order Black-Scholes formulas could be used to estimate parameters in the multi-factor Heston model to determine starting points for the optimization algorithm

Table 1: Descriptive statistics for the relative errors of Black-Scholes option price approximations evaluated on grid $\mathcal{M}$ in the case of the Heston model.

First-order Black-Scholes approximations in vol of vol $(C_{1,H},\ P_{1,H})$						
γ	mean_C	median_C	std_C	mean_P	median_P	std_P
0.01	1.8131e-6	0.000	2.1868e-6	1.8058e-6	0.000	2.2218e-6
0.05	4.2591e-5	3.1181e-5	3.7372e-5	4.2808e-5	3.1898e-5	3.3398e-5
0.15	3.7607e-4	2.7484e-4	3.2672e-4	3.7819e-4	2.8112e-4	2.9203e-4
0.25	1.0137e-3	7.4174e-4	8.7296e-4	1.0196e-3	7.5723e-4	7.8197e-4
0.5	3.6279e-3	2.6769e-3	3.0715e-3	3.6515e-3	2.6801e-3	2.7806e-3
Second-order Black-Scholes approximations in vol of vol $(C_{2,MH},\ P_{2,MH})$						
γ	mean_C	median_C	std_C	mean_P	median_P	std_P
0.01	2.7090e-9	0.000	8.7598e-8	2.3767e-9	0.000	7.1053e-8
0.05	3.3058e-7	0.000	9.9919e-7	2.9665e-7	0.000	9.1210e-7
0.15	8.6177e-6	2.9231e-6	1.9097e-5	8.0870e-6	2.8545e-6	1.6523e-5
0.25	3.9080e-5	8.7593e-6	8.5551e-5	3.6756e-6	9.2254e-6	7.4764e-5
0.5	2.8757e-4	6.0871e-5	6.1026e-4	2.7410e-4	6.5693e-5	5.5215e-4

Table 2: Some descriptive statistics for the call and put option prices evaluated on grid $\mathcal{M}$ in the case of Heston model.

γ	average call price	min call	max call	average put price	min put	max put
0.01	32.292	14.337	56.822	31.101	10.081	64.549
0.05	31.846	14.294	56.847	30.655	10.091	64.567
0.1	31.908	14.193	57.206	30.717	10.166	64.997
0.25	32.116	14.102	57.970	30.925	10.242	65.958
0.5	33.211	13.925	61.368	32.020	10.338	70.310

Table 3: Comparison of the time (seconds) required to compute 40,000 European call and put options using formulas (147) and (148) with the rectangular quadrature rule with N_p nodess ($Time_{true}$) and formulas $C_{2,H}$ (63) and $P_{2,H}$ (64) with $n = 1$ ($Time_{approx}$). The computation was made on an Intel CORE i7 (8th generation) processor.

N_p	2^2	2^4	2^7	2^{10}	2^{14}	2^{16}
Time_{true}(secs)	0.21	0.76	6.40	49.84	802.45	3210.95
Time_{approx}(secs)	0.0234					

Figure 1: Relative error distributions $e_{C,1} = |C_H - C_{1,H}|/|C_H|$ (upper panels) and $e_{P,1} = |P_H - P_{1,H}|/|P_H|$ (lower panels) when $\gamma = 0.15$ (left panels), $\gamma = 0.25$ (middle panels), and $\gamma = 0.5$ (right panels) obtained with first-order approximations $(C_{1,H}, P_{1,H})$.
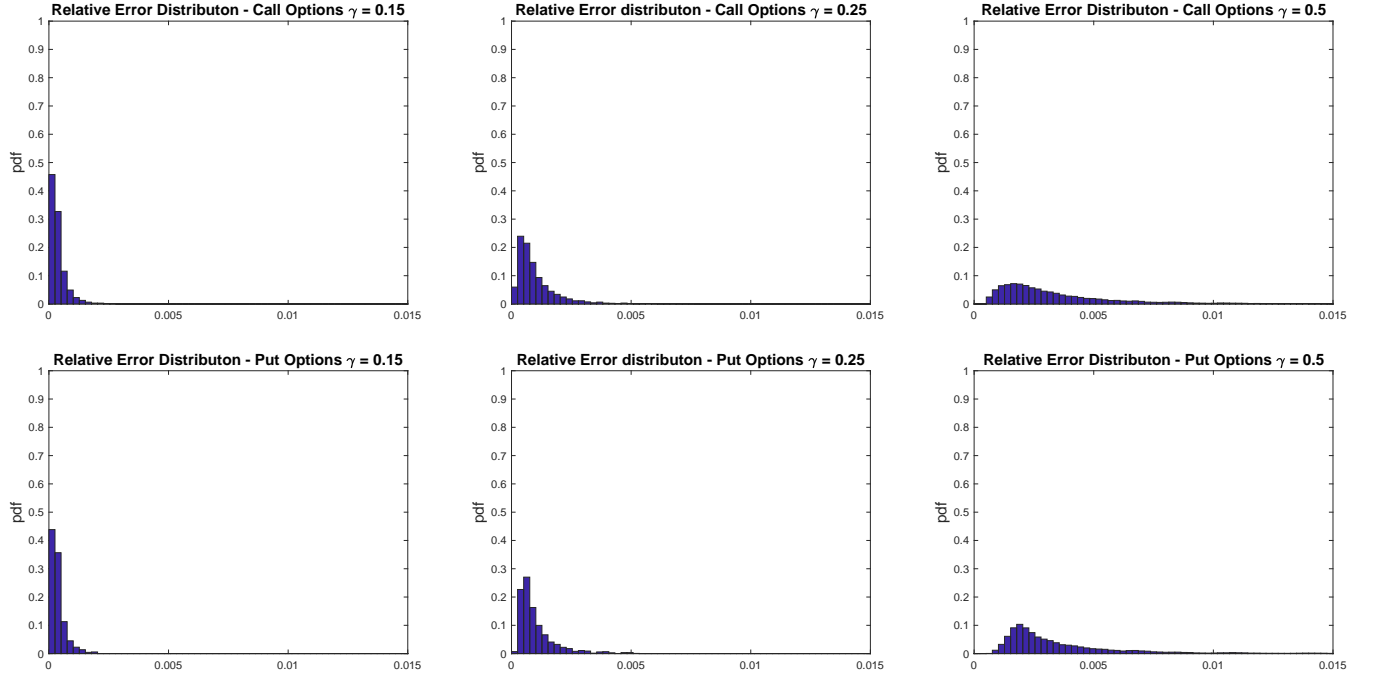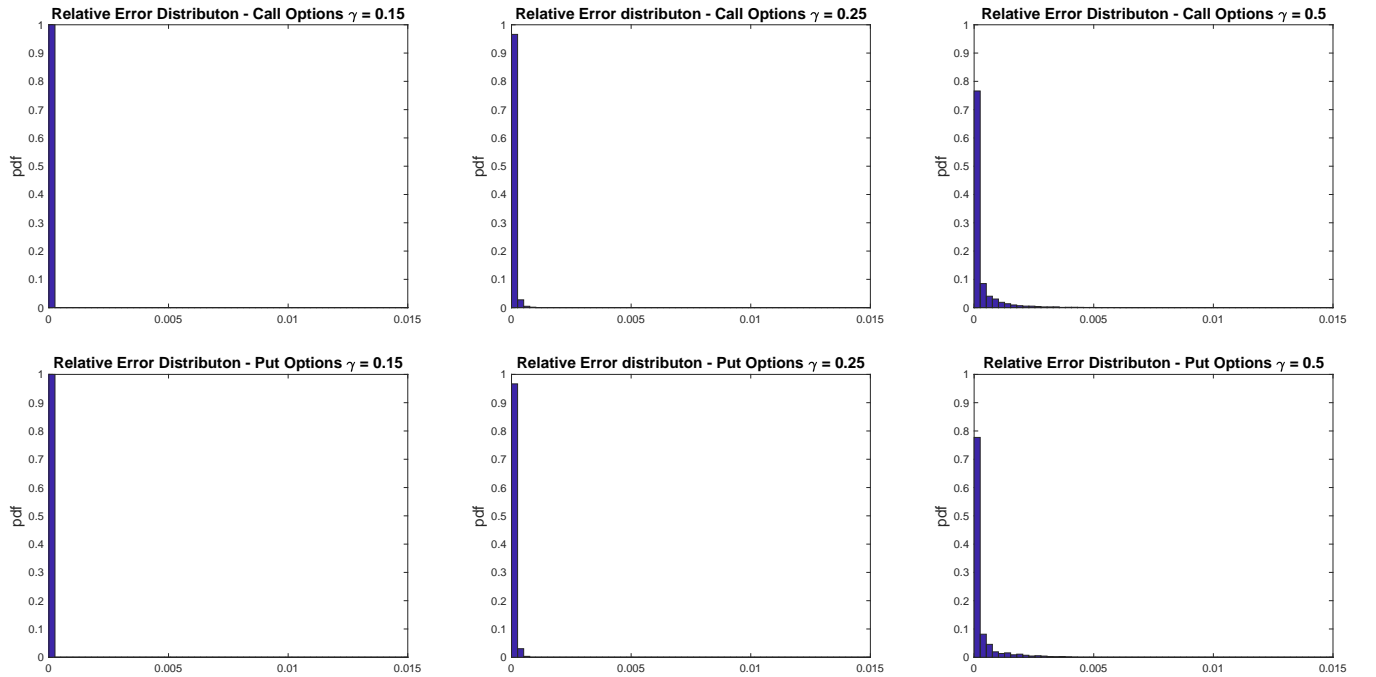

Figure 2: Relative error distributions $e_{C,2} = |C_H - C_{2,H}|/|C_H|$ (upper panels) and $e_{P,2} = |P_H - P_{2,H}|/|P_H|$ (lower panels) when $\gamma = 0.15$ (left panels), $\gamma = 0.25$ (middle panels), and $\gamma = 0.5$ (right panels) obtained with second-order approximations $C_{2,H}, P_{2,H}$.

used to solve the estimation problem.

17

4.2 Simulation study 2: Heston and double Heston with empirical parameters

In this subsection we investigate the quality of the approximations to the Heston and double Heston call and put option prices by comparing the second-order Black-Scholes formulas (63)–(64)) to Eqs. (147) and (148), when $n = 1, 2$ and model parameters calibrated to real data are used. Specifically we use the parameters estimated by Christoffersen et al. (2009). We report the values of these parameters in Tables 8 (Heston model) and 9 (double Heston model) in Appendix B. The last column of Tables 8 and the last two columns of 9 show that the Feller condition is violated in several cases. This means that the square root process can access zero with positive probability unless, as remarked in Christoffersen et al. (2009), the process satisfies a standard reflecting barrier at the origin. Interestingly, the Feller condition never holds in the case of process $v_{1,t}$. The violation of the Feller condition has also been noted in Pacati et al. (2018).

Table 4: Relative errors of European call and put options obtained by approximating the Heston/double Heston option prices with the second-order approximations (see formulas (63)–(64)), with model parameters from Table 8 for the Heston model and Table 9 for the double Heston model. Panel A shows the relative errors corresponding to the Heston model (H model), while Panel B shows those for the double Heston model (DH model). Risk free interest rate $r = 0.15$.

	T = 3 months				T = 6 months			
	Panel A		Panel B		Panel A		Panel B	
	Call	Put	Call	Put	Call	Put	Call	Put
	relative	relative	relative	relative	relative	relative	relative	relative
Year	errors	errors	errors	errors	errors	errors	errors	errors
	(H model)	(H model)	(DH model)	(DH model)	(H model)	(H model)	(DH model)	(DH model)
1990	0.00053	0.00048	0.00047	0.00066	0.00130	0.00141	0.00439	0.00502
1991	0.00016	0.00015	0.00709	0.00601	0.00037	0.00339	0.02427	0.02373
1992	0.00013	0.00013	0.11481	0.12308	0.00031	0.00037	0.19148	0.26218
1993	0.00010	0.00010	0.07643	0.07883	0.00023	0.00028	0.13649	0.18301
1994	0.00009	0.00010	0.24806	0.28858	0.00016	0.00024	0.31348	0.43928
1995	0.00011	0.00010	0.15384	0.16652	0.00027	0.00028	0.26902	0.37789
1996	0.00013	0.00011	0.00570	0.00468	0.00027	0.00029	0.01360	0.01571
1997	0.00016	0.00014	0.00249	0.00212	0.00038	0.00041	0.00577	0.00631
1998	0.00047	0.00046	0.00533	0.00426	0.00114	0.00134	0.01268	0.01525
1999	0.00037	0.00035	0.00447	0.00361	0.00085	0.00100	0.01090	0.01293
2000	0.00023	0.00021	0.00465	0.00380	0.00050	0.00059	0.01077	0.01247
2001	0.00022	0.00020	0.00448	0.00368	0.00038	0.00046	0.01022	0.01180
2002	0.00018	0.00018	0.00511	0.00419	0.00036	0.00047	0.01158	0.01343
2003	0.00025	0.00023	0.22127	0.25334	0.00064	0.00068	0.29631	0.41585
2004	0.00005	0.00005	0.00507	0.00414	0.00013	0.00018	0.01152	0.01339
Avg.	0.02%	0.02%	5.7%	6.7%	0.05%	0.05%	8.8%	12%

We compute the relative errors of the second-order approximations $C_{2,H}$, $P_{2,H}$ and $C_{2,DH}$ and $P_{2,DH}$ of the Heston/double Heston option prices for the value of the risk-free interest rate equal to 0.15 and for two time maturities: $T = 3$ months and $T = 6$ months. The spot variance of the Heston model is chosen to be 0.9, while the spot variances of the double Heston model are $v_1 = 0.13$ and $v_2 = 0.75$. This choice is supported by the results of the empirical analysis discussed in Christoffersen et al. (2009) p. 1926. In fact, in Christoffersen et al. (2009), the sum of the factor estimates $v_{1,0}$ and $v_{2,0}$ is 88% in the two-factor model and the difference is around 62% while it is 90% in the one-factor model.

Table 4 shows the results of this experiment for the Heston (Panel A) and double Heston (Panel B) models. We observe that, on average, for the shortest maturity $T = 3$ months, the relative errors are 0.02%

for both call and put options in the Heston framework and 5.7% and 6.7%, respectively, in the double Heston model. When the maturity is six months, the mean of the relative errors is 0.05% for both call and put options in the Heston model, while they are 8.8% and 12%, respectively, for the double Heston model. These relative errors guarantee four correct significant digits for the Heston model and two correct significant digits for the double Heston model.

It is worth noting that the largest relative errors for the double Heston model are obtained in the years 1992–1995 and 2003 when the vol of vol γ_1 is larger than 520%, with peaks of 943% in 1994 and 880% in 2003. In contrast to the double Heston model, the estimated vol of vol of the Heston model is always less than 80% and larger than 37% (see Tables 8 and 9). Bearing in mind these estimated values of vols of vols and noting that the correlation coefficients are less than -0.5, the relative errors shown in Table 4 could be considered satisfactory.

5   Performance of the Black-Scholes approximations: empirical analyses

This section presents two empirical exercises to assess the performance of our analytical approximation to reproduce the dynamics of the VIX index and to estimate Put and Call option prices one day ahead.

5.1   Variance of the Gaussian Kernel and the VIX index

In this subsection we asses the performance of the second-order variance Γ_2 in Eq. (31), of the Gaussian kernel behind the Heston and double Heston models, in reproducing the VIX dynamics when using data from S&P 500 index options.

To this end, we use the model parameters in Tables 8 and 9 corresponding to the years 2000, 2001, 2002, 2003 and the daily VIX data, along with realized variance time series of the S&P 500 in the same years[†].

For each fixed year, we use the model parameters in Tables 8 and 9 to compute the Kernel variance Γ_2 appearing in the Black-Scholes second order approximations Eqs. (63) and (64) and we use $\tilde{\Sigma}_{2,model}(t)$ to denote the quantity

$$\tilde{\Sigma}_{2,model}(t) = \sqrt{\frac{\Gamma_2(t, t+T)}{T}}, \quad model = H, DH, \tag{77}$$

where Γ_2 is given in (31) and T is chosen to be a calendar year (see Christoffersen et al. (2009) p. 1925). Thus, we denote this volatility by $\tilde{\Sigma}_{2,H}(t)$ or $\tilde{\Sigma}_{2,DH}(t)$ depending on whether we consider the Heston or double Heston model.

Specifically, for the Heston model, the realized variance from Oxford-Man Institute database plays the role of the spot variance, while in the double Heston model the realized variance is the sum of the two model variances (i.e., the variance of price log-return), while each variance is evaluated as a fraction, α, of this sum. The optimal value of α is computed by matching the first four sampled moments. In this specific experiment, let RV_t be the observed realized variance at time t. We choose $v_t = RV_t$ for the Heston model, while $v_{1,t} = \alpha RV_t$ and $v_{2,t} = (1 - \alpha)RV_t$ for the double Heston model. The optimal value of α is $\alpha = 0.06$ when we use the median truncated realized variance and $\alpha = 0.15$ in the case of 5-minute realized variance.

[†]The VIX level was downloaded from http://www.cboe.com/products/vix-index-volatility/vix-options-and-futures/vix-index/vix-historical-data, while the realized variance (median truncated realized variance and 5-minute realized variance) data are available from the Oxford-Man Institute website https://realized.oxford-man.ox.ac.uk/data .

The use of the realized variance as a short-term volatility factor is supported by the results illustrated in Corsi et al. (2013), which focused on realized volatility option pricing models.

Figures 3 and 4 show the VIX time series (solid line) and $\tilde{\Sigma}_{2,model}$ (dotted line) in the Heston (Fig. 3) and double Heston (Fig. 4) models as a function of the day index for each year considered.

Figures 3, and 4 shows that $\tilde{\Sigma}_{2,model}(t)$ (see Eq. (77)) is able to mimic closely the VIX behavior and that the double Heston model outperforms the Heston model in terms of the sup-norm as shown in Table 5. Bearing in mind that what follows is a rough comparison, the RMSE shown in Table 5 compares favorably with what is obtained by Corsi et al. (2013) (see Section 4.3, Table 4). This analysis provides further empirical evidence to support two already known findings: the ability of the double Heston model to capture the main features of market volatility — and the effect of the skewness in particular — and the use of RV as a proxy for unobservable volatility factors (see, for example, Corsi et al. (2013), Christoffersen et al. (2009), (2014)).
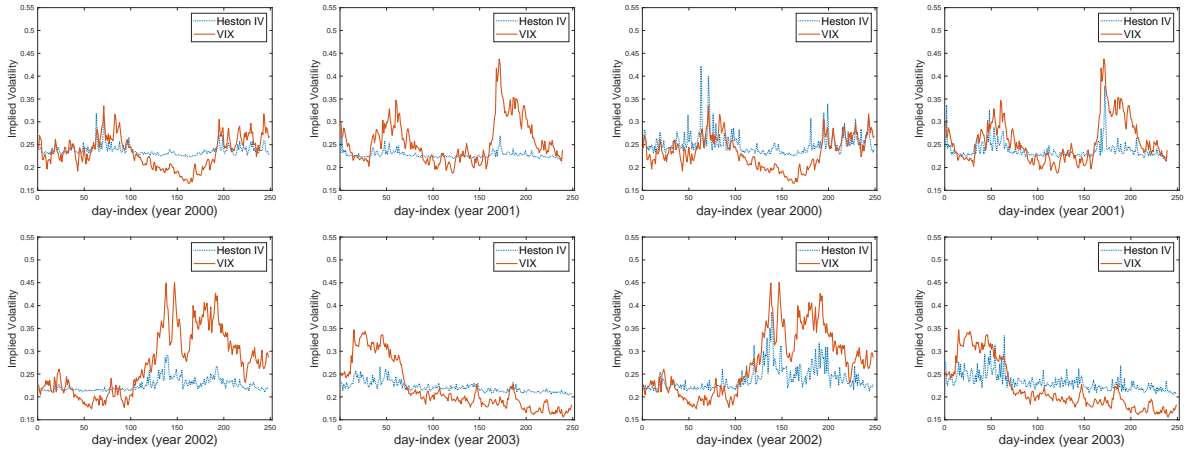

Figure 3: Each panel contains the VIX time series and the model implied volatility $\tilde{\Sigma}_{2,H}$ (i.e., Eq. (77) - Heston model) as a function of day. The model parameters in Table 8 were used with a spot variance of the price log-return corresponding to the daily time series of the median truncated realized variance (left panels) and the 5-minute realized variance (right panels) from the Oxford-Man Institute.

Table 5: Root Mean Square Error (RMSE) obtained using $\tilde{\Sigma}_{2,model}$ to approximate the VIX index.

Model	median truncated RV			5-minute RV		
	RMSE	min err	max err	RMSE	min err	max err
Heston	0.0276	0.0131	0.0453	0.0253	0.0168	0.0380
Double Heston	0.0239	0.0152	0.0341	0.0301	0.0233	0.0347

We then test for linear dependence between the VIX index and $\tilde{\Sigma}_{2,model}$ in Eq. (77) with $model = DH$ (i.e., $n = 2$) computed with the approach mentioned above. This is done by regressing the daily VIX observations only on the daily estimates of $\tilde{\Sigma}_{2,DH}(t)$. We use both the median truncated realized variance (see Table 6, left panel) and the 5-minute realized variance (see Table 6, right panel) as proxies of the stochastic variance processes as illustrated above.

The results of these zero-intercept regressions confirm our hypothesis that the second-order BS implied volatility in the Heston and multi-factor Heston models is able to capture VIX dynamics better than the naive linear model $VIX_t = \beta_1 RV_t + noise$. In fact, in the Heston and double Heston model, the coefficient
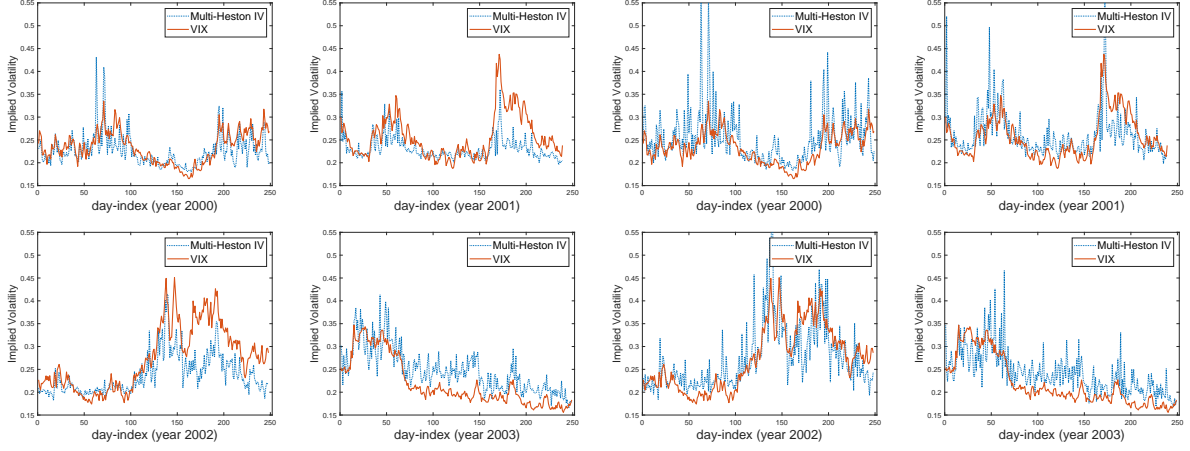
20

Figure 4: Each panel contains the VIX time series and the model implied volatility $\tilde{\Sigma}_{2,DH}$ (i.e., Eq (77) - Double Heston model) as a function of day. The model parameters in Table 9 were used with a spot variance of the price log-return corresponding to the daily time series of the median truncated realized variance (left panels, $\alpha = 0.15$) and the 5-minute realized variance (right panels, $\alpha = 0.06$) from the Oxford-Man Institute.

Table 6: Zero-intercept regression models with two proxies of stochastic variances. The model parameters are from Tables 3 in Christoffersen et al. 2009.

Proxy median truncated realized variance					Proxy 5-minute realized variance				
$VIX_t = \beta_1 RV_t + noise$					$VIX_t = \beta_1 RV_t + noise$				
year	β_1	S.E.	t-stat	R^2	$\tilde{\Sigma}_{2,DH}$ year	β_1	S.E.	t-stat	R^2
2000	0.589	0.0089	65.94	0.271	2000	0.807	0.0156	51.68	0.186
2001	0.490	0.0075	64.54	0.352	2001	0.706	0.0138	50.86	0.253
2002	0.574	0.0081	68.20	0.532	2002	0.784	0.0140	55.73	0.431
2003	0.524	0.0063	82.66	0.597	2003	0.671	0.0101	66.40	0.489
$VIX_t = \beta_1 \tilde{\Sigma}_{2,H}(t) + noise$					$VIX_t = \beta_1 \tilde{\Sigma}_{2,H}(t) + noise$				
year	β_1	S.E.	t-stat	R^2	year	β_1	S.E.	t-stat	R^2
2000	1.002	0.0075	132.2	0.600	2000	1.068	0.0080	132.2	0.602
2001	0.860	0.0092	92.67	0.553	2001	0.904	0.0088	102.3	0.599
2002	0.786	0.0102	76.65	0.599	2002	0.843	0.0098	85.254	0.646
2003	0.962	0.0120	80.17	0.591	2003	1.013	0.0121	83.488	0.609
$VIX_t = \beta_1 \tilde{\Sigma}_{2,DH}(t) + noise$					$VIX_t = \beta_1 \tilde{\Sigma}_{2,DH}(t) + noise$				
year	β_1	S.E.	t-stat	R^2	year	β_1	S.E.	t-stat	R^2
2000	0.9641	0.0072	132.6	0.599	2000	1.087	0.0120	90.56	0.410
2001	0.879	0.0079	110.74	0.635	2001	1.008	0.0106	94.51	0.557
2002	0.846	0.0080	105.18	0.732	2002	0.992	0.0112	88.14	0.655
2003	1.1092	0.0092	119.4	0.754	2003	1.107	0.0114	94.23	0.660

β_1 is, on average, equal to 0.90 and 0.94, respectively, in the left panel of Table 6, while it is, on average, 0.957 and 1.048, respectively, in the right panel. These coefficients are statistically significant at 5% levels. Furthermore, the coefficient of determination R^2 indicates that the second-order BS implied volatility model performs better than the naive models which use only RV_t as explanatory variable. <mark>These results are inline with findings in Huang et al. 2018.</mark>

5.2 Option price calibration

In this subsection we assess the performance of our Black & Scholes type formulas to reproduce the European call and put option prices on the US S&P 500 index. The U.S. three-month government bond index was used as a proxy for the interest rate r appearing in the Heston model. Figure 5 shows traded call (left panel) and put option (right panel) prices on the US S&P 500 index for various strike prices and expiry on December 19, 2015. We also provide empirical evidence that the Black-Scholes second-order approximations $C_{2,H}$ and
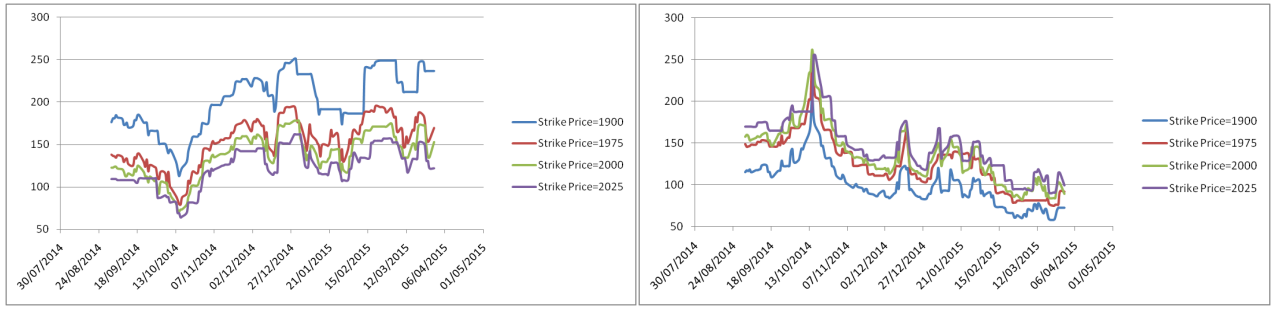

Figure 5: Prices of the call (left panel) and put (right panel) options on the U.S. S&P 500 index with strike prices $E_1 = 1900$, $E_2 = 1975$, $E_3 = 2000$, and $E_4 = 2025$ and with expiry date T = December 19, 2015, versus time (September 1, 2014 – March 30, 2015).

$P_{2,H}$ (see Eqs. (63)–(64)) and the implied volatility approximation $\Sigma_{2,H}$ in Eq. (70) are an efficient tool to obtain "consistent" estimates of the Heston model parameters. To this end, we propose a three-step procedure:

i) starting from the traded call option prices $C^o(S_i, T_i, E_j)$ with spot price S_i, time to maturity T_i and strike price E_j, and using the U.S. three-month government bond yield as risk-free interest rate, r, compute the observed implied volatility, $\sigma^o(S_i, T_i, E_j)$, $i = 1, 2, \ldots, n_T$, $j = 1, 2, \ldots, N_E$. This computation is done using the Matlab function *calcBSImpVol*, which uses Li's rational function approximator for the initial estimate (see, Li 2006; 2008), followed by Householder's root finder of the third order to improve the convergence rate of the Newton-Raphson method;

ii) for any time $i = 1, 2, \ldots, n_T$, estimate the Heston model parameters $\underline{\Theta}_i = (\gamma_i, v_i^*, \chi_i, \rho_i, v_0^i) \in \mathbb{R}^5$, $i = 1, 2, \ldots, n_T$, solving the following optimization problem:

$$\min_{\underline{\Theta} \in \mathcal{V}} \sum_{j=1}^{n_E} \left[\sigma^o(S_i, T_i, E_j) - \frac{\Sigma_{2,H}(S_i, T_i, E_j)}{\sqrt{T_i}} \right], \tag{78}$$

where $\Sigma_{2,MH}$ is given in formula (70) and $\mathcal{V}$ is the following set of constraints:

$$\mathcal{V} = \left\{ \underline{\Theta} = (\gamma, v^*, \chi, \rho, v_0) \in \mathbb{R}^5 \mid \gamma, v^*, \chi, v_0 > 0, \, -1 < \rho < 1 \right\}; \tag{79}$$

iii) compute the European call and put option prices using formulas $C_{2,H}$, $P_{2,H}$ in Eqs. (63)–(64) with the estimated parameters;

iv) evaluate the model consistency by computing the mean and standard deviation of the relative errors $E_{i,j}^C = |C^o(S_i, T_i, E_j) - C_{2,H}(S_i, T_i, E_j)|/C^o(S_i, T_i, E_j)$ and $E_{i,j}^P = |P^o(S_i, T_i, E_j) - P_{2,H}(S_i, T_i, E_j)|/P^o(S_i, T_i, E_j)$, where P^o is the observed value of the put option, $i = 1, 2, \ldots, n_T$, and $j = 1, 2, \ldots, n_E$.

v) repeat steps (i)–(iv) starting from the observed put prices $C^o(S_i, T_i, E_j)$, $i = 1, 2, \ldots, n_E$.

Table 7: Descriptive statistics for estimated values of the model parameters and observed implied volatility σ^o.

|				Call Set				
	χ	v^*	γ	ρ	v_0	$\frac{2\chi v^*}{\gamma^2}$	obj. func.	σ^o
mean	5.7999	0.014663	0.50098	-0.8502	0.08060	0.677512	8.35e-5	0.1581
median	5.7999	0.012726	0.50100	-0.8502	0.08200	0.588756	2.28e-5	0.1546
std	0.00057	0.007032	0.000303	0.000220	0.004912	0.324606	1.46e-4	0.020
				Put Set				
	χ	v^*	γ	ρ	v_0	$\frac{2\chi v^*}{\gamma^2}$	obj. func.	σ^o
mean	5.7999	0.029102	0.5009	-0.8502	0.08384	1.34530	7.84e-5	0.1931
median	5.7999	0.029114	0.5009	-0.8502	0.08489	1.29907	2.02e-5	0.1923
std	0.000020	0.006205	0.00026	0.00018	0.004243	0.28708	2.87e-4	0.0168
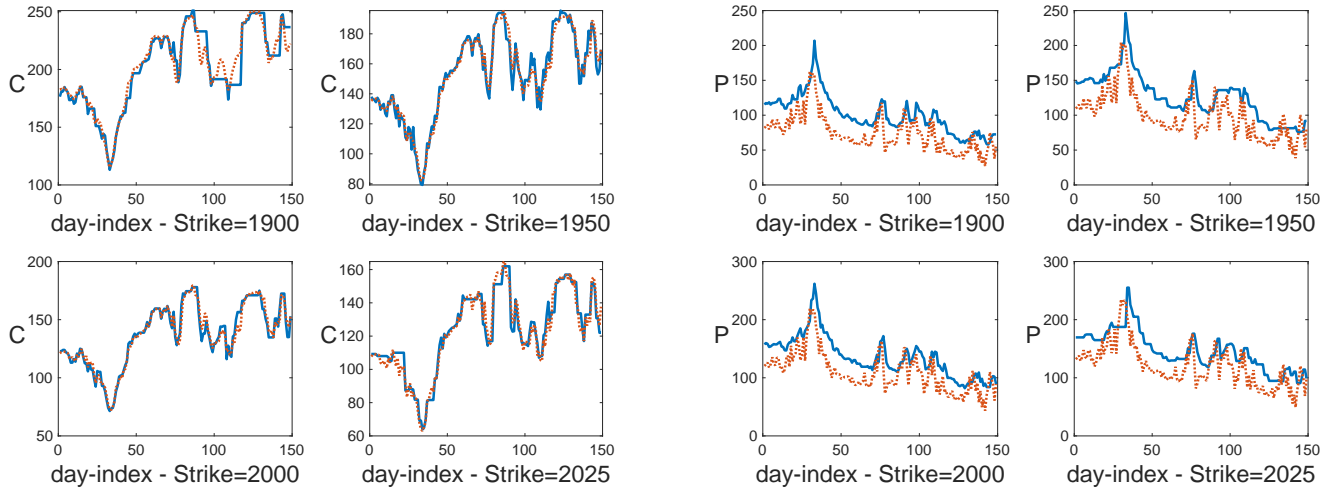
Figure 6: Left Panel: Observed call option prices (solid line) and the Black-Scholes second-order approximations $C_{2,H}$ (dotted line) for four different strike prices $E_1 = 1900$, $E_2 = 1975$, $E_3 = 2000$, and $E_4 = 2025$ and expiry date $T =$ December 19, 2015, versus time (September 1, 2014 – March 30, 2015) obtained with the optimal parameters from the observed implied volatility of call options (i.e. Call Set). Right Panel: Observed put option prices (solid line) and Black-Scholes second-order approximations $P_{2,H}$ (dotted line) for four different strike prices $E_1 = 1900$, $E_2 = 1975$, $E_3 = 2000$, and $E_4 = 2025$ and expiry date $T =$ December 19, 2015, versus time (September 1, 2014 – March 30, 2015) obtained with the optimal parameters from the observed implied volatility of call options (i.e. Call Set).

The use of the implied volatilities in the objective function (Eq. (78)) has two main advantages. First, satisfactory out-of-sample approximations of the implied volatilities may be useful to improve hedging strate-
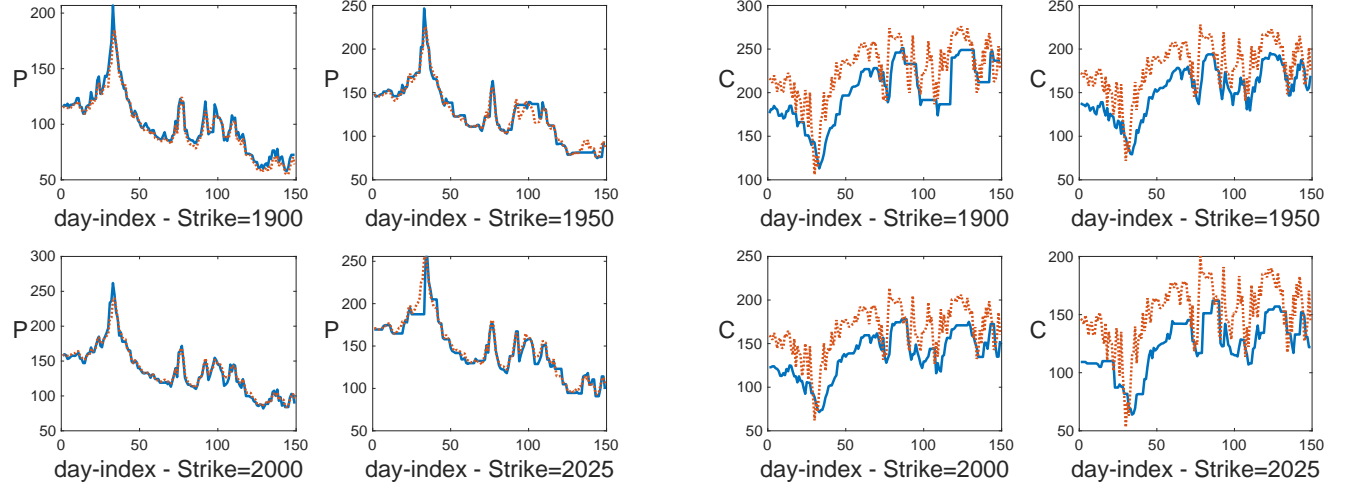
Figure 7: Left Panel: Observed put option prices (solid line), Black-Scholes second-order approximations $P_{2,H}$ (dotted line) for four different strike prices $E_1 = 1900$, $E_2 = 1975$, $E_3 = 2000$, and $E_4 = 2025$ and expiry date $T =$ December 19, 2015, versus time (September 1, 2014 – March 30, 2015) obtained with the optimal parameters from the observed implied volatility of put options (i.e. Put Set). Right Panel: Observed call option prices (solid line), Black-Scholes second-order approximations $C_{2,H}$ (dotted line) for four different strike prices $E_1 = 1900$, $E_2 = 1975$, $E_3 = 2000$, and $E_4 = 2025$ and expiry date $T =$ December 19, 2015, versus time (September 1, 2014 – March 30, 2015) obtained with the optimal parameters from the observed implied volatility of put options (i.e. Put Set).
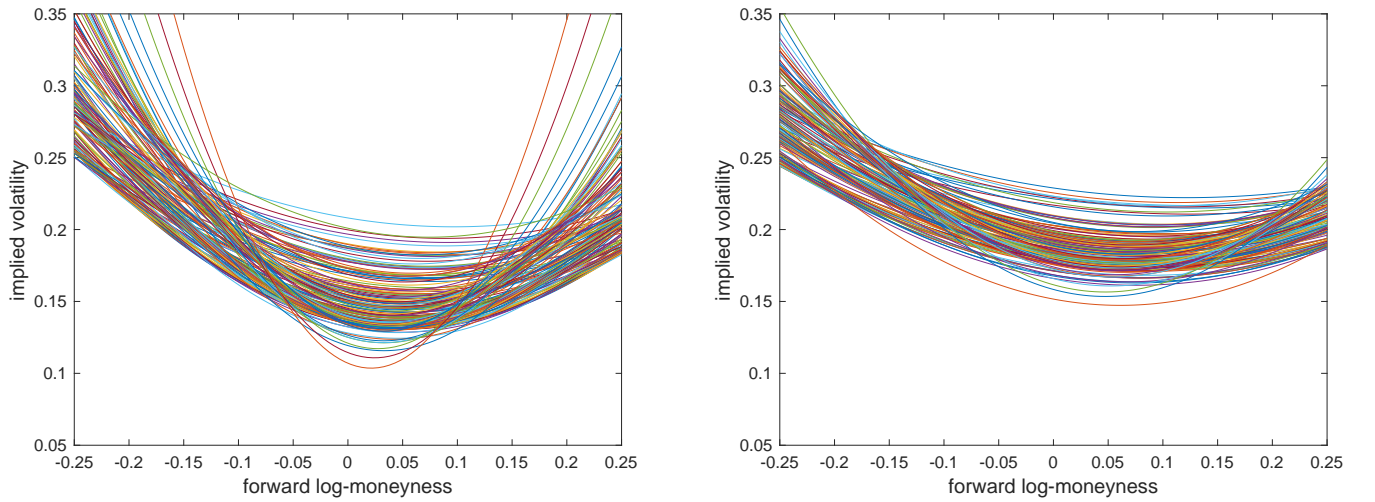

Figure 8: Implied volatility approximation $\Sigma_{2,H}$ as a function of the forward log-moneyness for all times to maturity obtained by using the optimal parameters Call Set (left) and Put Set (right). Period: September 1, 2014 – March 30, 2015.

gies. Second, estimating the model parameters by minimizing the implied volatilities avoids biased approximations caused by very different magnitudes of prices. In the empirical analysis we have four strike prices for call and put options (i.e., $n_E = 4$) and $n_T = 150$.

We use a metric variable steepest descent algorithm to solve problem (78) (see, for example, Recchioni and Scoccia (2000), Fatone et al. (2013)). This is an iterative algorithm which generates a sequence of points, $\underline{\Theta}^k$, $k = 0, 1, \ldots$, belonging to the interior of the feasible region and moving opposite to the gradient vectors of the objective function computed in a suitable metric.

Running this procedure, we obtain two optimal sets of model parameters, one obtained using the call options (Call Set) and the other using the put options (Put Set).
Some descriptive statistics for the estimated model parameters, initial variance, Feller ratio, and observed implied volatility are given for the two sets in Table 7. We observe that the main difference between the two sets is the estimates of the long-term mean. The difference in this parameter estimates is due to market imperfections that lead to a spread between the implied volatility σ^o of call and put options. In fact, the absolute value of the implied volatility spread is 0.04 on average while the relative absolute spread (i.e. the ratio of the spread to implied volatility from the call) is 0.24. Interestingly, the absolute difference between the square root of the two long term variances is 0.05 and the ratio of this difference to square root of the call variances is 0.29, thus mirroring the implied volatilty spread.
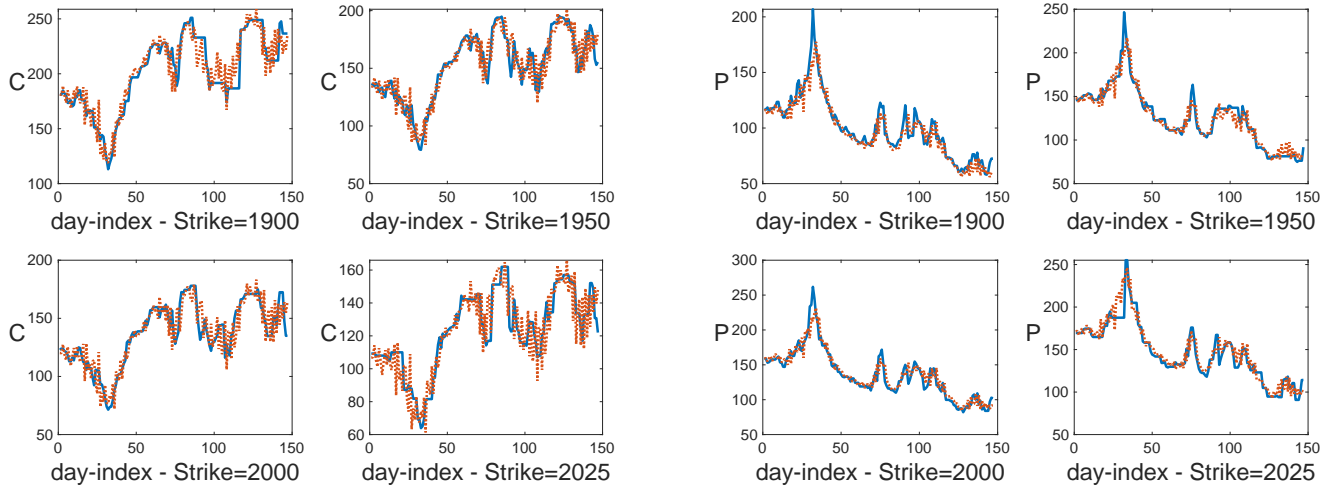

Figure 9: Observed option prices (solid line) and one-day ahead estimates computed using Black-Scholes second-order approximation (dotted line) for four different strike prices $E_1 = 1900$, $E_2 = 1975$, $E_3 = 2000$, and $E_4 = 2025$ and with expiry date $T =$ December 19, 2015, versus time (September 1, 2014 – March 30, 2015). Call price one-day ahead estimates using the Call Set (left panel); Put price one-day ahead using the Put Set (on the right). Average relative errors of call and put options: 7.9% and 6.2% respectively.

Figures 6 and 7 show the observed and Black-Scholes second-order (solid line and dotted line, respectively) call and put option prices. The approximations in Figure 6 are obtained using the model parameters estimated by the observed implied volatility from call options (i.e. Call Set) while those in Figure 7 are obtained using the model parameters estimated by the observed implied volatility from put options (i.e., Put set).
In Figure 6 the relative errors E^C are, on average, 0.027 (i.e., 2.7%) since we are using the Call Set. These

errors are inline with those in Pacati et al. 2018 where a double Heston with jump is used. By contrast, using the model parameters of the Call Set, the relative errors of the put options, E^P are, on average, 0.22 (i.e., 22%) which is compatible with the observed relative volatility spread of 0.24 (i.e., 24%).

When we use the Put Set to approximate the call and put option prices, we observe that the relative errors for the put options, E^P are, on average, 0.031 (i.e., 3.1%) while the relative errors for the call options E^C are, on average, 0.21 (i.e., 21%) inline with the observed relative volatility spread.
The volatility spread can be observed in Figure 8 which show the implied volatility approximations $\Sigma_{2,H}$ as a function of forward log-moneyness m_E (see Eq. (54)) for all times to maturity corresponding to the Call Set (left panel) and Put Set (right panel).

We conclude this section testing the potential of the calibrated parameters in estimating option prices one-day ahead. Figure 9 shows the one-day ahead estimates for call (left panel) and put (right panel) option prices. Specifically, the option estimates at time $t+1$ is carried out using the value of the optimal parameters at time t. The call one-day ahead estimated prices are obtained using the model parameters from the Call Set while the put one-day ahead estimated price from the Put Set. The relative errors of the one-day ahead estimates are, on average, 7.9% for the call option and 6.2% for the put options.

6   Conclusions

Although numerical methods for option pricing are extremely powerful in terms of accuracy, analytical approximations continue to be proposed for ease of use and to clearly connect the features of the model to the observed characteristics of the implied volatility surface. Along these lines, this paper presented an approach to extract the Gaussian behind the multi-factor Heston model that clearly connects the Black-Scholes framework to the multi-factor Heston framework. In detail, the Gaussian kernel which constitutes the "backbone" of the multi-factor Heston model allows for simple Black-Scholes-like option formulas and a simple expression for the implied volatility. The latter is able to explain well-known findings in the volatility smile. The main quantity responsible for the deviation from the Black-Scholes world is the price skewness; that is, S_1 is responsible for the smile asymmetry. For sufficiently large values of S_1, a non-convex volatility smile may be observed.

The simulation study and empirical analysis show that the second-order approximations for call and put options and the implied volatility approximation provide consistent results and a good approximation for the Heston option price formulas up to volatilities of volatilities on the order of 50%.

The results of this work suggest further investigations into the potential of the approximation for the Heston Greeks in several applications, such as portfolio management. As well, while the Black-Scholes formulas developed here could extend to the affine class of models without jumps, future work will entail developing a similar formula for affine models with jumps.

Appendix A: Proofs

Proof of Proposition 2.1

We recall the backward Kolmogorov equation satisfied by the function M given in (6) as a function of the

past log-price x and time t:

$$-\frac{\partial M}{\partial t} = \frac{1}{2}\sum_{j=1}^{n} v_j \frac{\partial^2 M}{\partial x^2} + \frac{1}{2}\sum_{j=1}^{n} \gamma_j^2 v_j \frac{\partial^2 M}{\partial v_j^2} + \sum_{j=1}^{n} \gamma_j \rho_j v_j \frac{\partial^2 M}{\partial x \partial v_j}$$

$$+ \sum_{j=1}^{n} \chi_j(v_j^* - v_j)\frac{\partial M}{\partial v_j} + \left(r(t) - \frac{1}{2}\sum_{j=1}^{n} v_j\right)\frac{\partial M}{\partial x} \tag{80}$$

with final condition

$$M(x,\underline{v},t',x',t') = \delta(x - x'), \tag{81}$$

where $\delta(\cdot)$ is the Dirac delta function. We look for M in the form

$$M(x,\underline{v},t,x',t') = \frac{1}{2\pi}\int_{-\infty}^{+\infty} e^{\imath k(x'-x)-\imath k \int_t^{t'} r(s)ds + A(k,t,t') - \sum_{j=1}^{n} v_j B_j(k,t,t')}dk,$$

$$M(x,\underline{v},t,x',t') = \frac{1}{2\pi}\int_{-\infty}^{+\infty} e^{\imath k(x'-x)) - \imath k \int_t^{t'} r(s)ds + Q(k,t,t';\underline{v},\underline{\Theta}_v)}dk,$$

$$x, x' \in \mathbb{R}, \ \underline{v} \in \mathbb{R}^{n^+}, \ t, t' \geq 0, t' - t > 0, \tag{82}$$

where Q is defined as

$$Q(t'-t,\underline{v},k;\underline{\Theta}_v) = A(k,t,t') - \sum_{j=1}^{n} v_j B_j(k,t,t'). \tag{83}$$

Substituting Eq. (83) into Eq. (80), we obtain the Riccati equation satisfied by A and B_j (see Duffie et al. 2000; Fatone et al. 2009):

$$\frac{d}{dt}A = \sum_{j=1}^{n} \chi_j v_j^* B_j, \tag{84}$$

and for $j = 1, 2, \ldots, n$,

$$\frac{d}{dt}B_j = \chi_j B_j + \frac{1}{2}\gamma_j^2 B_j^2 + \imath k \rho_j \gamma_j B_j - \frac{k^2}{2} + \frac{\imath k}{2}, \tag{85}$$

with final conditions

$$A(k,t',t') = 0, \ \ B_j(k,t',t') = 0, j = 1, 2, \ldots, n. \tag{86}$$

We now rewrite Q (Eq. (83)). Eqs. (84) and (86) give

$$A(k,t,t') = \sum_{j=1}^{n} A_j(k,t,t') = -\sum_{j=1}^{n} \chi_j v_j^* \int_t^{t'} B_j(k,\tau,t')d\tau, \tag{87}$$

where

$$A_j(k,t,t') = -\chi_j v_j^* \int_t^{t'} B_j(k,\tau,t')d\tau, \tag{88}$$

while Eqs. (85) and (86) give

$$\frac{d}{dt}\left(e^{-\chi_j t}B_j(k,t,t')\right) = e^{-\chi_j t}\left(\imath k \rho_j \gamma_j B_j(k,t,t') + \frac{1}{2}B_j^2(k,t,t')\right) + e^{-\chi_j t}\left(\frac{k^2}{2}-\imath\frac{k}{2}\right). \tag{89}$$

Integrating, we obtain

$$B_j(k,t,t') = -\int_t^{t'} e^{-\chi_j(s-t)}\left[\imath k \rho_j \gamma_j B_j(k,s,t') + \frac{1}{2}\gamma_j^2 B_j^2(k,s,t')\right] - \left(-\frac{k^2}{2}+\imath\frac{k}{2}\right)\int_t^{t'} e^{-\chi_j(s-t)}ds. \tag{90}$$

Using Eqs. (87) and (90), we obtain

$$A_j(k,t,t') - v_j B_j(k,t,t') =$$

$$v_j^*\chi_j \int_t^{t'}\int_\tau^{t'} e^{-\chi_j(s-t)}\left[\imath k \rho_j \gamma_j B_j(k,s,t') + \frac{1}{2}\gamma_j^2 B_j^2(k,s,t')\right]dsd\tau + \left(\frac{k^2}{2}-\imath\frac{k}{2}\right)v_j^*\chi_j\int_t^{t'}\int_\tau^{t'} e^{-\chi_j(s-t)}dsd\tau$$

$$+v_j\int_t^{t'} e^{-\chi_j(s-t)}\left[\imath k \rho_j \gamma_j B_j(k,s,t') + \frac{1}{2}\gamma_j^2 B_j^2(k,s,t')\right]ds + v_j\left(-\frac{k^2}{2}+\imath\frac{k}{2}\right)\int_t^{t'} e^{-\chi_j(s-t)}ds. \tag{91}$$

Inverting the integration order, we obtain

$$A_j(k,t,t') - v_j B_j(k,t,t') = +\left(\frac{k^2}{2}-\imath\frac{k}{2}\right)\int_t^{t'}\left[v_j^*\chi_j\int_t^\tau e^{-\chi_j(s-t)}d\tau\right]ds$$

$$+\int_t^{t'}\left[\imath k \rho_j \gamma_j B_j(k,s,t') + \frac{1}{2}\gamma_j^2 B_j^2(k,s,t')\right]\left[v_j^*\chi_j\int_t^\tau e^{-\chi_j(s-t)}d\tau\right]ds$$

$$+\left(-\frac{k^2}{2}+\imath\frac{k}{2}\right)\int_t^{t'} v_j e^{-\chi_j(s-t)}ds + \int_t^{t'}\left[\imath k \rho_j \gamma_j B_j(k,s,t') + \frac{1}{2}\gamma_j^2 B_j^2(k,s,t')\right]\left[v_j e^{-\chi_j(s-t)}\right]ds. \tag{92}$$

Bearing in mind that v_j is the variance at time t and that the conditional mean of the point-in-time volatility is

$$E(v_{j,s}\,|\,\mathcal{F}_t) = v_{j,t}e^{-\chi_j(s-t)} + v_j^*(1-e^{-\chi_j(s-t)}), \quad s \geq t, \tag{93}$$

Eq. (92) becomes

$$A_j(k,t,t') - v_j B_j(k,t,t') = \int_t^{t'}\left[\imath k \rho_j \gamma_j B_j(k,s,t') + \frac{1}{2}\gamma_j^2 B_j^2(k,s,t') + \left(-\frac{k^2}{2}+\imath\frac{k}{2}\right)\right]E(v_{j,s}\,|\,\mathcal{F}_t)ds. \tag{94}$$

Eq. (94) implies

$$\sum_{j=1}^n\left(A_j(k,t,t') - v_j B_j(k,t,t')\right) = -\frac{k^2}{2}\Gamma(t,t') + \frac{\imath k}{2}\Gamma(t,t') +$$

$$\sum_{j=1}^n\int_t^{t'} E(v_{j,s}\,|\,\mathcal{F}_t)\left[\frac{1}{2}\gamma_j^2 B_j^2(k,s,t') + \imath k \rho_j \gamma_j B_j(k,s,t')\right]ds, \tag{95}$$

where Γ is given in formula (13). This proves formulas (7) and (11). Formula (12) follows if we apply the convolution theorem for the inverse Fourier transform.

We now prove Eq. (8). First, we observe that B_j can be computed explicitly using a standard approach for the Riccati equations:

$$B_j = -\frac{2}{\gamma_j^2}\frac{\frac{d}{dt}C_j}{C_j}. \tag{96}$$

28

Substituting B_j into (85), we obtain

$$-\frac{2}{\gamma_j}\frac{\frac{d^2}{dt^2}C_j}{C_j} + \frac{2}{\gamma_j^2}\left(\frac{\frac{d}{dt}C_j}{C_j}\right)^2 = -\frac{2}{\gamma_j^2}(\chi_j + \imath k\rho_j\gamma_j)\frac{\frac{d}{dt}C_j}{C_j} + \frac{2}{\gamma_j^2}\left(\frac{\frac{d}{dt}C_j}{C_j}\right)^2 + \frac{1}{2}(-k^2 + \imath k), \qquad (97)$$

that is, C_j is the solution to the following initial value problem:

$$\frac{d^2}{dt^2}C_j - (\chi_j + \imath k\rho_j\gamma_j)\frac{d}{dt}C_j + \frac{\gamma_j^2}{4}(-k^2 + \imath k)C_j = 0, \qquad (98)$$

with initial conditions

$$C_j(k, t', t') = 1, \quad \frac{d}{dt}C_j(k, t', t') = 0. \qquad (99)$$

Solving problem (98), (99) we obtain

$$B_j(k, t, t') = \frac{1}{2}(k^2 - \imath k)\widetilde{B}_j(k, t, t'), \qquad (100)$$

where

$$\widetilde{B}_j(k, t, t') = \frac{1 - e^{-2\zeta_j(t'-t)}}{(\zeta_j + \nu_j) + (\zeta_j - \nu_j)e^{-2\zeta_j(t'-t)}}, \qquad (101)$$

in which ζ_j and ν_j are the quantities in Eqs. (9) and (10). Note that $\lambda_1 = \nu_j - \zeta_j$ and $\lambda_2 = \nu_j + \zeta_j$ are the complex roots of the characteristic equation associated with differential equation (98).
This concludes the proof. $\square$

Proof of Proposition 2.2

It is easy to see that the conditional marginal M in (6) can be rewritten as

$$M(x, \underline{v}, t, x', t') = \frac{1}{2\pi}\int_{-\infty}^{+\infty}\underbrace{e^{\imath k\left[(x'-x)-\int_t^{t'} r(s)ds + \frac{1}{2}\Gamma_1(t,t')\right] - \frac{1}{2}\Gamma_1(t,t')k^2}}_{Gaussian\,kernel}\underbrace{e^{\sum_{j=1}^n\int_t^{t'} E(v_{j,s}\,|\,\mathcal{F}_t)L_j(k,s,t')ds}}_{contribution\,from\,vols\,of\,vols}dk, \qquad (102)$$

where L_j is given by

$$L_j(k, s, t') = \frac{\gamma_j^2}{2}B_j^2(k, s, t') + \imath k\rho_j\gamma_j\left(B_j(k, s, t') + \frac{(\imath k + 1)}{2}\frac{\left(1 - e^{-\chi_j(t'-s)}\right)}{\chi_j}\right). \qquad (103)$$

Here, B_j, S_1, and Γ_1 are given in Eqs. (8), (19), and (20), respectively. Formula (102) follows by summing and subtracting the term $S_1(-k^2 + \imath k)$ in the exponent of the integrand in Eq. (11), where S_1 is given in Eq. (19).

Let us prove that the following expansion in powers of γ_j as $\gamma_j \to 0$, $j = 1, 2, \ldots, n$, holds:

$$L_j(k, s, t') = \imath k\rho_j\gamma_j\left(\frac{1}{2}(k^2 + 1)\frac{(1 - e^{-\chi_j(t'-s)})}{\chi_j}\right) + O(\gamma_j^2), \ \gamma_j \to 0. \qquad (104)$$

Using formulas (8) and (103), we have

$$B_j(k, s, t') = \frac{1}{2}(k^2 - \imath k)\frac{(1 - e^{-\chi_j(t'-s)})}{\chi_j} + O(\gamma_j), \gamma_j \to 0 \ s < t'. \qquad (105)$$

Eq. (105) follows from Eq. (85) if we neglect the terms that multiply powers of γ_j larger than zero, that is, by solving the problem

$$\frac{dB_{j,0}}{dt}(k,t,t') - \chi_j\, B_{j,0}(k,t,t') = -\frac{k^2}{2} + \frac{\imath\, k}{2} \tag{106}$$

with final condition

$$B_{j,0}(k,t',t') = 0. \tag{107}$$

The solution $B_{j,0}$ is the zero-order term of the expansion in powers of γ_j as γ_j approaches zero. It reads

$$B_{j,0}(k,t,t') = \frac{1}{2}\left(k^2 - \imath\, k\right)\frac{\left(1 - e^{-\chi_j(t'-t)}\right)}{\chi_j}. \tag{108}$$

Substituting Eq. (105) into Eq. (103) and bearing in mind that we are interested only in the first two terms (zero and first order) in the expansion of L_j as γ_j approaches zero, we obtain

$$
\begin{aligned}
L_j(k,s,t') &= \frac{\gamma_j^2}{2}B_j^2(k,s,t') + \imath\, k\rho_j\gamma_j\left(\frac{1}{2}(k^2 - \imath k)\frac{(1 - e^{-\chi_j(t'-s)})}{\chi_j} + O(\gamma_j) + \frac{(\imath k + 1)}{2}\frac{(1 - e^{-\chi_j(t'-s)})}{\chi_j}\right) \\
&= \frac{\gamma_j^2}{2}B_j^2(k,s,t') + \imath\, k\rho_j\gamma_j\left(\frac{k^2}{2}\frac{(1 - e^{-\chi_j(t'-s)})}{\chi_j} + O(\gamma_j) + \frac{1}{2}\frac{(1 - e^{-\chi_j(t'-s)})}{\chi_j}\right) \\
&= \frac{1}{2}\frac{\rho_j\gamma_j}{\chi_j}(1 - e^{-\chi_j(t'-s)})\left(\imath k^3 + \imath k\right) + O(\gamma_j^2),\ \gamma_j \to 0^+.
\end{aligned} \tag{109}
$$

This proves formula (104).

Substituting L_j with $\frac{1}{2}\frac{\rho_j\gamma_j}{\chi_j}(1 - e^{-\chi_j(t'-s)})\left(\imath k^3 + \imath k\right)$ in formula (102) and using the convolution theorem for the inverse Fourier transform, we obtain formula (18).

This concludes the proof. $\square$

Proof of Proposition 2.3

We start by proving Eqs. (24) and (25). To this end, we rewrite M_1 in (23) as follows:

$$M_1(x,\underline{v},t,x',t') = \mathcal{G}_{MH}(x' - x,t,t') + \int_{-\infty}^{+\infty}\mathcal{G}_{MH}(x' - x - y,t,t')\left[\frac{S_1(t,t')}{2\pi}\int_{-\infty}^{+\infty}e^{\imath k y}\left(\imath\, k + \imath\, k^3\right)\right]dk\,dy. \tag{110}$$

Integrating Eq. (110), we have:

$$
\begin{aligned}
\int_{-\infty}^{+\infty}M_1(x,\underline{v},t,x',t')dx' &= 1 + \int_{-\infty}^{+\infty}\left[\frac{S_1(t,t')}{2\pi}\int_{-\infty}^{+\infty}e^{\imath k y}\left(\imath\, k + \imath\, k^3\right)\right]dk\,dy \\
&= 1 + S_1(t,t')\int_{-\infty}^{+\infty}\delta(k)\left(\imath\, k + \imath\, k^3\right)dk = 1.
\end{aligned} \tag{111}
$$

Likewise,

$$
\begin{aligned}
\int_{-\infty}^{+\infty}e^{x'}M_1(x,\underline{v},t,x',t')dx' &= e^x + e^x\int_{-\infty}^{+\infty}\left[\frac{S_1(t,t')}{2\pi}\int_{-\infty}^{+\infty}e^{\imath y(k-\imath)}\left(\imath\, k + \imath\, k^3\right)\right]dk\,dy \\
&= e^x + S_1(t,t')e^x\int_{-\infty}^{+\infty}\delta(k - \imath)\left(\imath\, k + \imath\, k^3\right)dk = e^x.
\end{aligned} \tag{112}
$$

We now prove formula (110), that is, formula (23). The latter is obtained from Eq. (18) using a suitable expansion of the Airy function as the vol of vol goes to zero. In fact, when $\gamma_j \to 0$, $j = 1, 2, \ldots, n$ we have $S_1 \to 0$. We use the following expansion of $\mathcal{A}_{S_1}$ as a function of S_1 when S_1 approaches zero:

$$
\begin{aligned}
\mathcal{A}_{S_1}(y) &= \frac{1}{2\pi} \int_{-\infty}^{+\infty} e^{\imath k y} e^{S_1(t,t')(\imath k^3 + \imath k)} dk \\
&= \frac{1}{2\pi} \int_{-\infty}^{+\infty} e^{\imath k y} \left(1 + S_1(t,t')(\imath k^3 + \imath k) + O(S_1^2(t,t')) \right) dk, \ S_1 \to 0.
\end{aligned}
\tag{113}
$$

Thus, Eq. (113) gives

$$
\mathcal{A}_{S_1}(y) = \delta(y) + S_1(t,t') \left(\delta'(y) - \delta'''(y) \right) + o\left(\|\underline{\gamma}\| \right), \ \|\underline{\gamma}\| \to 0,
\tag{114}
$$

where $\delta(\cdot)$ is the Dirac delta function and $\delta'(\cdot)$ and $\delta'''(\cdot)$ are its first- and third-order derivatives. Substituting Eq. (114) into Eq. (18) and using the definition of the derivatives of the Dirac delta function, we have

$$
M(x, \underline{v}, t, x', t') = \mathcal{G}_{MH}(x' - x, t, t') + S_1(t,t') \left[-\frac{d}{dy} + \frac{d^3}{dy^3} \right] \mathcal{G}_{MH}(x' - x - y, t, t') \bigg|_{y=0} + o\left(\|\underline{\gamma}\| \right),
$$
$$
\|\underline{\gamma}\| \to 0.
\tag{115}
$$

Eq. (115) and the fact that $\frac{d^j}{dy^j} \mathcal{G}_\Gamma = (-1)^j \frac{d^j}{dx'^j} \mathcal{G}_\Gamma$ implies (23).

We conclude by proving Eq. (26). We compute

$$
\int_{-\infty}^{+\infty} \left(x' - x - \int_t^{t'} r(s) + \frac{1}{2}\Gamma_0(t,t') \right) M_1(x, \underline{v}, t, x', t') dx'
$$
$$
\int_{-\infty}^{+\infty} \left(x' - x - \int_t^{t'} r(s) + \frac{1}{2}\Gamma_0(t,t') - S_1(t,t') \right) \mathcal{G}_{\Gamma_1}(x' - x, t, t') dx' \ + \ S_1(t,t')
$$
$$
+ S_1(t,t') \int_{-\infty}^{+\infty} \left(x' - x - \int_t^{t'} r(s) + \frac{1}{2}\Gamma_0(t,t') \right) \left[-\frac{d^3 \mathcal{G}_{\Gamma_1}}{dx'^3}(x' - x, t, t') + \frac{d\mathcal{G}_{\Gamma_1}}{dx'}(x' - x, t, t') \right] dx'.
\tag{116}
$$

The thesis follows by integrating by parts and bearing in mind that $\Gamma_1 = \Gamma_0 - 2S_1$ and

$$
\int_{-\infty}^{+\infty} \left(x' - x - \int_t^{t'} r(s) + \frac{1}{2}\Gamma_1(t,t') \right) \mathcal{G}_{\Gamma_1}(x' - x, t, t') dx' = 0.
$$

This concludes the proof. $\square$

Proof of Proposition 2.4

It is easy to see that the conditional marginal M in (6) can be rewritten as

$$
M(x, \underline{v}, t, x', t') = \frac{1}{2\pi} \int_{-\infty}^{+\infty} \underbrace{e^{\imath k \left[(x' - x) - \int_t^{t'} r(s) ds + \frac{1}{2}\Gamma_2(t,t') \right] - \frac{1}{2}\Gamma_2(t,t')k^2}}_{Gaussian\,kernel} \underbrace{e^{\sum_{j=1}^n \int_t^{t'} E(v_{j,s} \,|\, \mathcal{F}_t) R_j(k,s,t') ds}}_{contribution\,from\,vols\,of\,vols} dk,
\tag{117}
$$

31

where R_j is given by

$$R_j(k, s, t') =$$
$$\frac{\gamma_j^2}{2}\left(B_j^2(k,s,t') + \frac{(k^2 - \imath k)}{4}\left(\frac{1 - e^{-\chi_j(t'-s)}}{\chi_j}\right)^2\right) + \imath\, k\rho_j\gamma_j\left(B_j(k,s,t') + \frac{(\imath k + 1)}{2}\left(\frac{1 - e^{-\chi_j(t'-s)}}{\chi_j}\right)\right).$$

(118)

Here, B_j is given in Eq. (8), and Γ_2 is defined in Eq. (31). Formula (117) follows by summing and subtracting the term $(-S_1(t,t') + S_2(t,t'))(-k^2 + \imath k)$ in the exponent of the integrand in Eq. (11), where S_1 is given in Eq. (19).

We prove that the following expansion in powers of γ_j as $\gamma_j \to 0$, $j = 1, 2, \ldots, n$, holds:

$$R_j(k, s, t') = \frac{\gamma_j^2}{2}(k^4 - 2\imath k^3 - \imath k)\frac{\psi_j^2(s,t')}{4} + \frac{\gamma_j^2\rho_j^2}{2\chi_j}(k^4 - \imath k^3)\psi_j(s,t')f_j(s,t')$$
$$+ \frac{\rho_j\,\gamma_j}{2}(\imath k^3 + \imath k)\psi_j(s,t') + o(\gamma_j^2), \quad \gamma_j \to 0,$$

(119)

where ψ_j and f_j are given by:

$$\psi_j(t, t') = \frac{(1 - e^{-\chi_j(t'-t)})}{\chi_j}, \quad t < t',$$

(120)

and

$$f_j(t, t') = \left(\psi_j(t' - t) - (t' - t)e^{-\chi_j(t'-t)}\right) = e^{-\chi_j(t'-t)}\int_t^{t'}(e^{\chi_j(t'-s)} - 1)ds \quad t < t'.$$

(121)

To this end, we prove the following expansion for B_j (8):

$$B_j(k, t, t') = B_{j,0}(k, t, t') + \gamma_j B_{j,1}(k, t, t') + O(\gamma_j^2), \quad \gamma_j \to 0^+, \quad t < t'.$$

(122)

The zero-order term of the expansion, $B_{j,0}$ is given in Eq. (107) while the first-order term is the solution of the following problem:

$$\frac{dB_{j,1}}{dt}(k, t, t') - \chi_j B_{j,1}(k, t, t') = \imath\, k\, \rho_j B_{j,0}(k, t, t'),$$

(123)

with final condition $B_{j,1}(k, t', t') = 0$. Thus, $B_{j,1}$ is

$$B_{j,1}(k, t, t') = -\frac{\imath\, k\, \rho_j}{2\chi_j}\left(k^2 - \imath k\right)f_j(t, t').$$

(124)

Using Eq. (122) in Eq. (118), we have

$$R_j(k, s, t') = \frac{\gamma_j^2}{2}\left(B_0^2(k, s, t') + \frac{(k^2 - \imath k)}{4}\psi_j^2(s, t')\right)$$
$$+ \imath\, k\rho_j\gamma_j\left(B_{j,0}(k, s, t') + \gamma_j B_{j,1}(k, s, t') + \frac{(\imath k + 1)}{2}\psi_j(s, t')\right) + o(\gamma_j^2), \gamma_j \to 0^+,$$

(125)

which also reads as

$$R_j(k, s, t') = \frac{\gamma_j^2}{2}\left(\frac{\psi_j^2(s, t')}{4}(k^2 - \imath k)^2 + \frac{(k^2 - \imath k)}{4}\psi_j^2(s, t')\right)$$
$$+ \imath\, k\rho_j\gamma_j\left(\frac{\psi_j(s, t')}{2}(k^2 - \imath k) + \frac{\gamma_j\rho_j}{2\chi_j}f_j(s, t')(-\imath k^3 - k^2) + \frac{(\imath k + 1)}{2}\psi_j(s, t')\right) + o(\gamma_j^2), \gamma_j \to 0^+.$$

(126)

The expansion (119) follows from (126) with a simple computation.

Using expansion (119) in (117) we obtain

$$M(x, \underline{v}, t, x', t') = \frac{1}{2\pi} \int_{-\infty}^{+\infty} \underbrace{e^{\imath k \left[(x'-x) - \int_t^{t'} r(s)ds + \frac{1}{2}\Gamma_2(t,t') \right] - \frac{1}{2}\Gamma_2(t,t')k^2}}_{Gaussian\,kernel} \times$$

$$\underbrace{e^{\sum_{j=1}^n \int_t^{t'} E(v_{j,s} \mid \mathcal{F}_t) \left[\frac{\gamma_j^2}{2}(k^4 - 2\imath k^3 - \imath k)\frac{\psi_j^2(s,t')}{4} + \frac{\gamma_j^2 \rho_j^2}{2\chi_j}(k^4 - \imath k^3)\psi_j(s,t')f_j(s,t') + \frac{\rho_j \gamma_j}{2}(\imath k^3 + \imath k)\psi_j(s,t') + o(\gamma_j^2) \right] ds}}_{contribution\,from\,vols\,of\,vols} \, dk,$$

(127)

that is,

$$M(x, \underline{v}, t, x', t') = \frac{1}{2\pi} \int_{-\infty}^{+\infty} \underbrace{e^{\imath k \left[(x'-x) - \int_t^{t'} r(s)ds + \frac{1}{2}\Gamma_2(t,t') \right] - \frac{1}{2}\Gamma_2(t,t')k^2}}_{Gaussian\,kernel} \times$$

$$\underbrace{e^{S_1(0,T)(\imath k^3 + \imath k) + S_2(0,T)(k^4 - 2\imath k^3 - \imath k) + S_{2c}(0,T)(k^4 - \imath k^3) + o(\|\underline{\gamma}\|^2)}}_{contribution\,from\,vols\,of\,vols} \, dk,$$

(128)

where S_1 is a linearly homogeneous function of the vols of vols while S_2 and S_{2c} are homogeneous function of degree two.

We compute the first three terms of the expansion in powers of the vols of vols of the function

$$\mathcal{E}(\underline{\gamma}) = e^{S_1(0,T)(\imath k^3 + \imath k) + S_2(0,T)(k^4 - 2\imath k^3 - \imath k) + S_{2c}(0,T)(k^4 - \imath k^3)}. \tag{129}$$

Formula (28) follows bearing in mind that we have:

$$\left. \frac{\partial \mathcal{E}}{\partial \gamma_j} \right|_{\underline{\gamma}=\underline{0}} = (\imath k^3 + \imath k)\frac{\partial S_1}{\partial \gamma_j}, \tag{130}$$

$$\left. \frac{\partial^2 \mathcal{E}}{\partial \gamma_j \gamma_i} \right|_{\underline{\gamma}=\underline{0}} = (\imath k^3 + \imath k)^2 \frac{\partial S_1}{\partial \gamma_i} \frac{\partial S_1}{\partial \gamma_j}, \; i \neq j, \tag{131}$$

and

$$\left. \frac{\partial^2 \mathcal{E}}{\partial \gamma_j^2} \right|_{\underline{\gamma}=\underline{0}} = (\imath k^3 + \imath k)^2 \left(\frac{\partial S_1}{\partial \gamma_j} \right)^2 + \frac{\partial^2 S_2}{\partial \gamma_j^2}(k^4 - 2\imath k^3 - \imath k) + \frac{\partial^2 S_{2c}}{\partial \gamma_j^2}(k^4 - \imath k^3). \tag{132}$$

This concludes the proof since Eqs. (32)–(34) can be proven as in Proposition 2.2. $\square$

Proof of Proposition 3.1

The price of a European vanilla call option with maturity T, spot price S_0, and strike price E discounted by a deterministic factor $B(T)$ is given in Eq. (44). Thus, using formula (22) for M in (44), we have

$$C(S_0, T, E) = B(T) \int_{\log E}^{+\infty} (e^{x'} - E)\mathcal{G}_{\Gamma_1}(x' - \log S_0, 0, T)dx'$$

$$+ B(T)S_1(0,T) \int_{\log E}^{+\infty} (e^{x'} - E) \left[-\frac{d^3 \mathcal{G}_{\Gamma_1}}{dx'^3}(x' - \log S_0, t, t') + \frac{d\mathcal{G}_{\Gamma_1}}{dx'}(x' - \log S_0, t, t') \right] dx' + o\left(\|\underline{\gamma}\| \right),$$

$$\|\underline{\gamma}\| \to 0. \tag{133}$$

Formula (51) follows by integrating by parts. Formula (52) is obtained in a similar way. That is, we have

$$P(S_0, T, E) = B(T) \int_{-\infty}^{\log E} (E - e^{x'}) \mathcal{G}_{\Gamma_1}(x' - \log S_0, 0, T) dx'$$

$$+ B(T) S_1(0, T) \int_{-\infty}^{\log E} (E - e^{x'}) \left[-\frac{d^3 \mathcal{G}_{\Gamma_1}}{dx'^3}(x' - \log S_0, t, t') + \frac{d \mathcal{G}_{\Gamma_1}}{dx'}(x' - \log S_0, t, t') dx' \right] + o\left(\|\underline{\gamma}\| \right),$$

$$\|\underline{\gamma}\| \to 0. \tag{134}$$

The correction $\mathcal{R}_{1,MH}$ for the call option is the same as the put correction since there are two changes of sign: one due to the payoff function and the other due to integration by parts over the interval $(-\infty, \log E)$ rather than $(\log E, +\infty)$. This concludes the proof. $\square$

Proof of Proposition 3.2

The price of a European vanilla call option with maturity T, spot price S_0, and strike price E discounted by a deterministic factor $B(T)$ is given in Eq. (44). Thus, using formula (27) for M in (44), we have

$$C(S_0, T, E) = B(T) \int_{\log E}^{+\infty} (e^{x'} - E) \mathcal{G}_{\Gamma_2}(x' - \log S_0, 0, T) dx'$$

$$+ B(T) S_1(0, T) \int_{\log E}^{+\infty} (e^{x'} - E) \left[-\frac{d^3 \mathcal{G}_{\Gamma_2}}{dx'^3} + \frac{d \mathcal{G}_{\Gamma_2}}{dx'} \right] (x' - \log S_0, 0, T) dx'$$

$$+ S_2(0, T) \int_{\log E}^{+\infty} (e^{x'} - E) \left[\frac{d^4 \mathcal{G}_{\Gamma_2}}{dx'^4} + 2\frac{d^3 \mathcal{G}_{\Gamma_2}}{dx'^3} - \frac{d \mathcal{G}_{\Gamma_2}}{dx'} \right] (x' - \log S_0, 0, T) dx'$$

$$+ S_{2c}(0, T) \int_{\log E}^{+\infty} (e^{x'} - E) \left[\frac{d^4 \mathcal{G}_{\Gamma_2}}{dx'^4} + \frac{d^3 \mathcal{G}_{\Gamma_2}}{dx'^3} \right] (x' - \log S_0, 0, T) dx'$$

$$+ \frac{1}{2} S_1^2(0, T) \int_{\log E}^{+\infty} (e^{x'} - E) \left[\frac{d^6 \mathcal{G}_{\Gamma_2}}{dx'^6} - 2\frac{d^4 \mathcal{G}_{\Gamma_2}}{dx'^4} + \frac{d^2 \mathcal{G}_{\Gamma_2}}{dx'^2} \right] (x' - \log S_0, 0, T) dx + o\left(\|\underline{\gamma}\| \right), \|\underline{\gamma}\| \to 0. \tag{135}$$

As mentioned above, the notation $[\cdot](\cdot, \cdot, \cdot)$ means that the function in the square parentheses is evaluated at $(\cdot, \cdot, \cdot)$. Formula (57) follows by integrating by parts.

Proceeding in a similar manner, we obtain the approximation for the put option in Eq. (58). As mentioned above, the correction $\mathcal{R}_{2,MH}$ for the call option is the same as the put correction since there are two changes of sign: one due to the payoff function and the other due to integration by parts over the interval $(-\infty, \log E)$ rather than $(\log E, +\infty)$.
This concludes the proof. $\square$

Proof of Proposition 3.3

Let us prove formula (68).
When $\underline{\gamma} = \underline{0}$ (i.e., all vols of vols equal zero), we have $\Gamma_1(0, T)$ equal to $\Gamma_0(0, T)$ and the correction term $\mathcal{R}_{1,MH}$ equal to zero, which implies

$$\Sigma_{1,MH}(\underline{0}) = \sqrt{\Gamma_0(0, T)}. \tag{136}$$

We compute the partial derivative of both sides of equation (66) with respect to γ_j, $j = 1, 2, \ldots, n$ and we evaluate the derivatives at $\underline{\gamma} = \underline{0}$. Using the Black-Scholes Vega (i.e., $\frac{\partial C_{BS}}{\partial \sigma}|_{\underline{\gamma}=\underline{0}} = S_0 N'(d_1(\Gamma_0))\sqrt{T}$, Eq.

(56)), and the derivatives of Γ_1 and S_1 with respect to γ_j, we have

$$\frac{\partial C_{BS}}{\partial \sigma}\bigg|_{\underline{\gamma}=\underline{0}} \frac{\partial}{\partial \gamma_j} \Sigma_{1,MH}(\underline{0}) = \frac{\rho_j\, \mathcal{T}_j(0,T)}{2\chi_j} S_0 N'(d_1(\Gamma_0)) \left[-\frac{1}{\sqrt{\Gamma_0(0,T)}} - d_2(\Gamma_0) + \frac{1}{\sqrt{\Gamma_0(0,T)}} \right],$$
(137)

where

$$\mathcal{T}_j(t,t') = \int_t^{t'} \left(1 - e^{-\chi_j(t'-s)} \right) E(v_{j,s}\,|\,\mathcal{F}_t) ds,$$
(138)

while d_1 and d_2 are given in Eqs. (49) and (50).

Eq. (137) and the expression for the Black-Scholes Vega, $\frac{\partial C_{BS}}{\partial \sigma}|_{\underline{\gamma}=\underline{0}} = S_0 N'(d_1(\Gamma_0))\sqrt{T}$, yield the derivative $\frac{\partial}{\partial \gamma_j} \Sigma_{1,MH}$ at $\underline{\gamma} = \underline{0}$:

$$\frac{\partial}{\partial \gamma_j} \Sigma_{1,MH}\bigg|_{\underline{\gamma}=\underline{0}} = \frac{\rho_j\, \mathcal{T}_j(0,T)}{2\chi_j} \frac{1}{\sqrt{\Gamma_0(0,T)}} \left(+\frac{1}{2} - \frac{(\ln(S_0/E) + \int_0^T r(s)ds)}{\Gamma_0(0,T)} \right),$$
(139)

thus implying

$$\Sigma_{1,MH}(\underline{\gamma}) = \sqrt{\Gamma_0(0,T)} - \frac{1}{\sqrt{\Gamma_0(0,T)}} \left(\frac{(\ln(S_0/E) + \int_0^T r(s)ds)}{\Gamma_0(0,T)} - \frac{1}{2} \right) \sum_{j=1}^n \frac{\gamma_j \rho_j}{2\chi_j} \mathcal{T}_j(0,T) + o\left(\|\underline{\gamma}\|\right), \quad \|\underline{\gamma}\| \to 0.$$
(140)

We now prove Eq. (70).
We observe that Eq. (70) can be rewritten as

$$\Sigma_{2,MH}(\underline{\gamma}) = \Sigma_{1,MH}(\underline{\gamma}) + \Sigma_{2,c}(\underline{\gamma}),$$
(141)

where $\Sigma_{2,c}(\underline{\gamma})$ is the contribution to the second-order approximation due to the second-degree powers of vols of vols:

$$\Sigma_{2,c}(\underline{\gamma}) = \frac{1}{2} \frac{S_1^2}{\Gamma_0\sqrt{\Gamma_0}} \left[(1 - \frac{6}{\Gamma_0})(m_E + \frac{1}{2}\Gamma_0)^2 + (\frac{3}{\Gamma_0} - 1)(m_E + \frac{1}{2}\Gamma_0) + \frac{2}{\Gamma_0} \right)$$
$$\frac{S_2}{\Gamma_0\sqrt{\Gamma_0}} \left[\frac{(m_E + \frac{1}{2}\Gamma_0)^2}{\Gamma_0} - (m_E + \frac{1}{2}\Gamma_0) - 1 \right] + \frac{S_{2c}}{\Gamma_0\sqrt{\Gamma_0}} \left[\frac{(m_E + \frac{1}{2}\Gamma_0)^2}{\Gamma_0} - 1 \right].$$
(142)

The derivation of the linear approximation $\Sigma_{1,MH}$ is the same as above. In order to derive the second-order term of the expansion of Σ in powers of vols of vols (i.e., Σ_{2c}), we need to compute the second-order derivatives of Σ with respect the vols of vols. We have

$$\frac{1}{T} \frac{\partial^2 C_{BS}}{\partial \sigma^2}\bigg|_{\underline{\gamma}=\underline{0}} \left(\frac{\partial \Sigma}{\partial \gamma_j} \right)^2\bigg|_{\underline{\gamma}=\underline{0}} + \frac{1}{\sqrt{T}} \frac{\partial C_{BS}}{\partial \sigma}\bigg|_{\underline{\gamma}=\underline{0}} \frac{\partial^2}{\partial \gamma_j^2} \Sigma_{2,MH}(\underline{0}) =$$

$$= \frac{1}{T} \frac{\partial^2 C_{BS}}{\partial \sigma^2}\bigg|_{\underline{\gamma}=\underline{0}} \left(\frac{\partial S_1}{\partial \gamma_j} \right)^2 \frac{1}{\Gamma_0} \left[-\frac{2}{\Gamma_0}(m_E + \frac{1}{2}\Gamma_0) - 1 \right] + \frac{1}{\sqrt{T}} \frac{\partial C_{BS}}{\partial \sigma}\bigg|_{\underline{\gamma}=\underline{0}} \frac{1}{\Gamma_0^{3/2}} \left(\frac{\partial S_1}{\partial \gamma_j} \right)^2 \times$$

$$\left[-1 + \frac{6}{\Gamma_0}(m_E + \frac{1}{2}\Gamma_0) + \frac{(m_E + \frac{1}{2}\Gamma_0)^4}{\Gamma_0^3} + \frac{(m_E + \frac{1}{2}\Gamma_0)^3}{\Gamma_0^2} - (\frac{6}{\Gamma_0} + 1)\frac{(m_E + \frac{1}{2}\Gamma_0)}{\Gamma_0} + (\frac{3}{\Gamma_0} + 1)[1 - (m_E + \frac{1}{2}\Gamma_0)] \right]$$

$$+ \frac{\partial^2 S_2}{\partial \gamma_j^2} \frac{Vega(\Gamma_0)}{\sqrt{T}\,\Gamma_0^{3/2}} \left[\frac{(m_E + \frac{1}{2}\Gamma_0)^2}{\Gamma_0} - (m_E + \frac{1}{2}\Gamma_0) - 1 \right] + \frac{\partial^2 S_{2c}}{\partial \gamma_j^2} \frac{Vega(\Gamma_0)}{\sqrt{T}\,\Gamma_0^{3/2}} \left[\frac{(m_E + \frac{1}{2}\Gamma_0)^2}{\Gamma_0} - 1 \right]$$
(143)

and

$$\frac{1}{T} \left.\frac{\partial^2 C_{BS}}{\partial \sigma^2}\right|_{\underline{\gamma}=\underline{0}} \left(\frac{\partial \Sigma}{\partial \gamma_j}\right) \left.\left(\frac{\partial \Sigma}{\partial \gamma_i}\right)\right|_{\underline{\gamma}=\underline{0}} + \frac{1}{\sqrt{T}} \left.\frac{\partial C_{BS}}{\partial \sigma}\right|_{\underline{\gamma}=\underline{0}} \frac{\partial^2}{\partial \gamma_j \partial \gamma_i} \Sigma_{2,MH}(\underline{0}) =$$

$$= \frac{1}{T} \left.\frac{\partial^2 C_{BS}}{\partial \sigma^2}\right|_{\underline{\gamma}=\underline{0}} \left(\frac{\partial S_1}{\partial \gamma_j}\right) \left(\frac{\partial S_1}{\partial \gamma_i}\right) \frac{1}{\Gamma_0} \left[-\frac{2}{\Gamma_0}(m_E + \frac{1}{2}\Gamma_0) - 1 \right] + \frac{1}{\sqrt{T}} \left.\frac{\partial C_{BS}}{\partial \sigma}\right|_{\underline{\gamma}=\underline{0}} \frac{1}{\Gamma_0^{3/2}} \left(\frac{\partial S_1}{\partial \gamma_j}\right) \left(\frac{\partial S_1}{\partial \gamma_i}\right) \times$$

$$\left[-1 + \frac{6}{\Gamma_0}(m_E + \frac{1}{2}\Gamma_0) + \frac{(m_E + \frac{1}{2}\Gamma_0)^4}{\Gamma_0^3} + \frac{(m_E + \frac{1}{2}\Gamma_0)^3}{\Gamma_0^2} - (\frac{6}{\Gamma_0} + 1)\frac{(m_E + \frac{1}{2}\Gamma_0)}{\Gamma_0} + (\frac{3}{\Gamma_0} + 1)[1 - (m_E + \frac{1}{2}\Gamma_0)] \right].$$

$$(144)$$

Bearing in mind that we have

$$\left.\frac{\partial C_{BS}}{\partial \sigma}\right|_{\underline{\gamma}=\underline{0}} = Vega(\Gamma_0) \tag{145}$$

and

$$\left.\frac{\partial^2 C_{BS}}{\partial \sigma^2}\right|_{\underline{\gamma}=\underline{0}} = Vomma(\Gamma_0) = Vega(\Gamma_0)\frac{\sqrt{T}}{\Gamma_0^{3/2}}(m_E + \frac{1}{2}\Gamma_0)(m_E - \frac{1}{2}\Gamma_0), \tag{146}$$

an easy but involved computation show that the addenda containing powers of $(m_E + \frac{1}{2}\Gamma_0)$ higher than two are canceled by the addenda involving the Black-Scholes Vomma.

This concludes the proof. $\square$

Appendix B: Formulas from Recchioni and Sun (2016) and Tables from Christoffersen et al. (2009)

The Recchioni and Sun (2016) formulas read as

$$C_{MH}(S_0, T, E) = e^{(q-1)\int_0^T r(s)ds} \frac{S_0}{2\pi} \int_{-\infty}^{+\infty} \frac{\left(\frac{S_0}{E}\right)^{(q-1-\imath k)} e^{-\imath k \int_0^T r(s)ds} e^{Q_{v,q}(T, v_0, k; \underline{\Theta}_v)}}{-k^2 - (2q-1)\imath k + q(q-1)} dk,$$

$$T > 0, S_0, \ v_0 > 0, \ q > 1, \tag{147}$$

and

$$P_{MH}(S_0, T, E) = e^{(q-1)\int_0^T r(s)ds} \frac{S_0}{2\pi} \int_{-\infty}^{+\infty} \frac{\left(\frac{S_0}{E}\right)^{(q-1-\imath k)} e^{-\imath k \int_0^T r(s)ds} e^{Q_{v,q}(T, v_0, k; \underline{\Theta}_v)}}{-k^2 - (2q-1)\imath k + q(q-1)} dk,$$

$$T > 0, S_0, \ v_0 > 0, \ q < 0, \tag{148}$$

where, in the case of the Heston/double Heston model, $Q_{v,q}$ is the elementary function given by

$$Q_{v,q}(t'-t, v, k; \underline{\Theta}_v) = \sum_{j=1}^{n} -(2\chi_j v_j^*/\gamma_j^2) \ln(s_{q,v_j,b}/(2\zeta_{q,v_j}))$$

$$-(2\chi v_j^*/\gamma_j^2)(\zeta_{q,v_j} + \mu_{q,v_j})(t'-t) - (2v_j/\gamma_j^2)(\zeta_{q,v_j}^2 - \mu_{q,v_j}^2)s_{q,v_j,g}/s_{q,v_j,b}, \tag{149}$$

with μ_{q,v_j}, ζ_{q,v_j}, $s_{q,v_j,g}$, and $s_{q,v_j,b}$ defined as follows:

$$\mu_{q,v_j} = -\frac{1}{2}\left(\chi_j + (\imath\, k - q)\,\gamma_j\,\rho_j\right), \tag{150}$$

$$\zeta_{q,v_j} = \frac{1}{2}\left[4\mu_{q,v_j}^2 + 2\gamma_j^2\varphi_q(k)\right]^{1/2}, \tag{151}$$

$$s_{q,v_j,g} = 1 - e^{-2\zeta_{q,v_j}(t'-t)}, \tag{152}$$

$$s_{q,v_j,b} = (\zeta_{q,v_j} + \mu_{q,v_j})e^{-2\zeta_{q,v_j}(t'-t)} + (\zeta_{q,v_j} - \mu_{q,v_j}). \tag{153}$$

The quantity φ_q in Eq. (150) is given by

$$\varphi_q(k) = \frac{k^2}{2} + \imath\frac{k}{2}(2q-1) - \frac{1}{2}(q^2 - q),\ k \in \mathbb{R}. \tag{154}$$

Table 8: Estimated parameters, one-factor stochastic volatility model (see Panel A, Table 3 in Christoffersen et al. (2009)).

year	χ	v^*	γ	ρ	$\frac{2\chi\,v^*}{\gamma^2}$
1990	1.9561	0.0593	0.8516	-0.6717	0.3198
1991	2.4240	0.0442	0.5834	-0.6957	0.6295
1992	2.5476	0.0375	0.5519	-0.6865	0.6272
1993	2.6846	0.0254	0.5105	-0.6703	0.5233
1994	4.4324	0.0233	0.4560	-0.8519	0.9933
1995	2.5070	0.0190	0.5597	-0.5061	0.3041
1996	3.1798	0.0298	0.5823	-0.5619	0.5589
1997	2.1672	0.0528	0.6018	-0.5666	0.6319
1998	1.8315	0.1029	0.8079	-0.7521	0.5774
1999	2.1310	0.1091	0.7552	-0.7404	0.8152
2000	2.5751	0.0678	0.6561	-0.6975	0.8111
2001	3.8191	0.0564	0.6489	-0.7410	1.0231
2002	3.3760	0.0532	0.5973	-0.7725	1.0068
2003	1.7201	0.0691	0.6837	-0.5939	0.5085
2004	1.6048	0.0464	0.3796	-0.7670	1.0335

Table 9: Estimated parameters, two-factor stochastic volatility model (see Panel B, Table 3 in Christoffersen et al. (2009)).

year	χ_1	v_1^*	γ_1	ρ_1	χ_2	v_2^*	γ_2	ρ_2	$\frac{2\chi_1 v_1^*}{\gamma_1^2}$	$\frac{2\chi_2 v_2^*}{\gamma_2^2}$
1990	0.2370	0.0227	1.0531	-0.7695	8.4983	0.0273	0.6827	-0.8417	0.0097	0.9955
1991	0.2966	0.0197	1.8157	-0.8575	4.4513	0.0319	0.3360	-0.6057	0.0035	2.5.155
1992	0.2022	0.0051	6.2755	-0.9670	0.7424	0.0684	0.2740	-0.8040	0.0001	1.3527
1993	0.2000	0.0052	5.2500	-0.9666	0.6131	0.0569	0.2123	-0.8216	0.0001	1.5480
1994	0.1668	0.0050	9.4346	-0.9877	0.2098	0.1633	0.1706	-0.9364	0.0000	2.3543
1995	0.2061	0.0050	6.8941	-0.9206	1.4677	0.0242	0.2413	-0.7512	0.0000	1.2200
1996	0.2101	0.0052	2.0149	-0.9684	0.5561	0.0575	0.1868	-0.7978	0.0005	1.8327
1997	0.1397	0.0053	1.5423	-0.9914	0.1878	0.1648	0.1239	-0.8928	0.0006	4.0321
1998	0.1374	0.0051	2.1196	-0.9917	0.6247	0.1733	0.3965	-0.9117	0.0003	1.3772
1999	0.1388	0.0051	1.9895	-0.9917	0.7322	0.1736	0.3828	-0.9108	0.0003	1.7372
2000	0.1404	0.0052	1.9382	-0.9915	0.3542	0.1690	0.2292	-0.9024	0.0004	2.2789
2001	0.1433	0.0054	1.9115	-0.9911	0.2347	0.1655	0.2047	-0.8983	0.0004	1.8539
2002	0.1491	0.0058	1.9754	-0.9902	0.1855	0.1607	0.1715	-0.8896	0.0004	2.0270
2003	0.1638	0.0032	8.8078	-0.9838	0.4625	0.1198	0.3976	-0.6569	0.0000	0.7009
2004	0.1500	0.0059	1.9829	-0.9902	0.2335	0.1621	0.1971	-0.8918	0.0005	1.9486

References

[1] Abadir, K.M., and Rockinger, M. 2003. Density functionals with an option-pricing application. Econometric Theory 19 (5): 778-811.

[2] Aït-Sahalia, Y. 2002. Maximum likelihood estimation of discretely sampled diffusions: a closed-form approximation approach. Econometrica 70 (1): 223-262.

[3] Benhamou, E., Gobet, E. and Miri, M. 2009. Smart expansion and fast calibration for jump diffusions. Finance and Stochastics 13 (4): 563-589.

[4] Berestycki, H., Busca, J., and Florent, I. 2004. Computing the implied volatility in stochastic volatility models. Communications on Pure and Applied Mathematics 57(10): 1352-1373.

[5] Bollen, N., Whaley, R. E. 2004. Does Net Buying Pressure Affect the Shape of Implied Volatility Functions?. The Journal of Finance 59 (2): 711-753.

[6] Christoffersen, P., Heston, S., and Jacobs, K. 2009. The shape and term structure of the index option smirk: Why multifactor stochastic volatility models work so well. Management Science 55: 1914-1932.

[7] Christoffersen, P., Feunou, B., Jacobs, K., and Meddahi, N. 2014. The economic value of realized volatility: using high-frequency returns for option valuation. Journal of Financial and Quantitative Analysis 49(3): 663-697.

[8] Corsi, F., Fusari, N., and La Vecchia, D. 2013. Realizing smiles: options pricing with realized volatility. Journal of Financial Economics 107: 284-304.

[9] Craig, W., and Goodman, J. 1990. Linear dispersive equation of Airy type. Journal of Differential Equations 87, 38-61.

[10] Cui, Y., del Bano Rollin, S., Germano G. 2017. Full and fast calibration of the Heston stochastic volatility model. European Journal of Operational Research 263(2), 625-638.

[11] Das, S. R., Sundaram, R. K. (1999). Of smiles and smirks: A term-structure perspective. Journal of Financial and Quantitative Analysis, 34(2), 211-240.

[12] Drimus, G.G. 2011. Closed-form convexity and cross-convexity adjustments for Heston prices. Quantitative Finance 11(8), 1137-1149.

[13] Duffie, D., Pan, J., and Singleton, K. 2000. Transform analysis and asset pricing for affine jump diffusions. Econometrica 68, 1343–1376.

[14] Egorov, A.V., Li, H., and Xu, Y. 2003. Maximum likelihood estimation of time-inhomogeneous diffusions. Journal of Econometrics 114 (1), 107-139.

[15] Fatone, L., Mariani, F., Recchioni, M.C., and Zirilli, F. 2009. An explicitly solvable multi-scale stochastic volatility model: option pricing and calibration. Journal of Futures Markets 29(9), 862-893.

[16] Fatone, L., Mariani, F., Recchioni, M.C., and Zirilli, F. 2013. The analysis of real data using a multiscale stochastic volatility model. European Financial Management 19(1), 153-179 .

[17] Feunou, B., and Okou, C. 2017. Good volatility, bad volatility, and option pricing. Journal Financial and Quantitative Analysis, forthcoming.

[18] Fouque, J.P., Papanicolaou, G., and Sircar, K.R. 2000. Derivatives in Financial Markets with Stochastic Volatility. Cambridge University Press.

[19] Friz, P.K. , Gerhold, S., Gulisashvili, A., and Sturm, S. 2011. On refined volatility smile expansion in the Heston model. Quantitative Finance

[20] Hagan, P.S., Kumar, D., Lesniewski, A.S., and Woodward, D.E. 2002. Managing smile risk. Wilmott Magazine, 84-108.

[21] Heston, S.L. 1993. A closed-form solution for options with stochastic volatility with applications to bond and currency options. The Review of Financial Studies 6, 327–343.

[22] Huang, D., Schlag, C., Shaliastovich, I., Thimme, J. 2018. Volatility-of-Volatility risk. Journal of Financial and Quantitative Analysis. Forthcoming.

[23] Kristensen, D., and Mele, A. 2011. Adding and subtracting Black-Scholes: a new approach to approximating derivative prices in continuous-time models. Journal of Financial Economics 102, 390–415.

[24] Larsson, K. 2012. General approximation schemes for option prices in stochastic volatility models. Quantitative Finance 12 (6), 873-891.

[25] Lee, R.W. 2001. Implied and local volatilities under stochastic volatility. International Journal of Theoretical and Applied Finance 4 (1), 45-89.

[26] Lewis, A.L. 2000. Option Pricing Under Stochastic Volatility, with Mathematica Code. Finance Press. ISBN: 0967637201.

[27] Li, M. 2006. You Don't Have to Bother Newton for Implied Volatility (November, 2006). Available at SSRN: https://ssrn.com/abstract=952727 or http://dx.doi.org/10.2139/ssrn.952727

[28] Li, M. 2008. Approximate Inversion of the Black-Scholes Formula Using Rational Functions. European Journal of Operational Research 185(2), 743–759.

[29] Lorig, M., Pagliarini, S., and Pascucci, A. 2017. Explicit implied volatilities for multifactor local-stochastic volatility models. Mathematical Finance 27(3), 926-960.

[30] Medvedev, A., and Scaillet, O. 2007. Approximation and calibration of short-term implied volatilities under jump-diffusion stochastic volatility. Review of Financial Studies 20(2), 427-459.

[31] Nicolato, N., and Sloth, D. 2012. Approximation of option prices under time-changed dynamics. Working Paper, Aarhus University.

[32] Pacati, C., Renó, R., Pompa, G. 2018. Smiling twice: the Heston++ model. Journal of Banking and Finance 96, 185-206.

[33] Recchioni, M.C., and Scoccia, A. 2000. A stochastic algorithm for constrained global optimization. Journal of Global Optimization 16, 257-270.

[34] Recchioni, M.C., and Sun, Y. 2016. An explicitly solvable Heston model with stochastic interest rate. European Journal of Operational Research 249, 359-377.

[35] Recchioni, M.C., and Tedeschi, G. 2017. From bond yield to macroeconomic instability: A parsimonious affine model. European Journal of Operational Research 262 (3), 1116-1135.

[36] Revuz, D. and M. Yor, M. 1991. Continuous Martingales and Brownian Motion, Fundamental Principles of Mathematical Sciences. vol. 293, Springer, Berlin.

[37] Sloth, D. 2013. Smile expansions. Available at: `http://econ.au.dk/fileadmin/Economics_Business/Research/Seminars/2013/DaviSloth_-_SmileExpansions.pdf`..

[38] Zhang, J.E., Zhen, F., Sun, X., Zhao, H. (2017). The skewness implied in the Heston model and its application. Journal of Futures Markets 37(3), 211-237.

[39] Vallée, O., and Soares, M. 2004. Airy Functions and Applications to Physics, Imperial College Press, London, distributed by World Scientific, Singapore, 2004.

[40] Yu, J. 2007. Closed-form likelihood approximation and estimation of jump-diffusions with an application to the realignment risk of the Chinese yuan. Journal of Econometrics 141 (2), 1245-1280.